Open access • Posted Content • DOI:10.1101/2020.08.25.267484

The Population Genetics of Collateral Resistance and Sensitivity — Source link

Sarah M. Ardell, Sergey Kryazhimskiy

Institutions: University of California, San Diego

Published on: 22 Aug 2021 - bioRxiv (Cold Spring Harbor Laboratory)

Topics: Population

The Population Genetics of Pleiotropy, and the Evolution of Collateral Resistance and Sensitivity in Bacteria

Sarah M. Ardell[1], Sergey Kryazhimskiy[1*]

1 Division of Biological Sciences, University of California San Diego, La Jolla, CA 92093

*Corresponding author: skryazhi@ucsd.edu

Abstract

Pleiotropic fitness tradeoffs and their opposite, buttressing pleiotropy, underlie many important phenomena in ecology and evolution. Yet, predicting whether a population adapting to one ("home") environment will concomitantly gain or lose fitness in another ("non-home") environment remains challenging, especially when adaptive mutations have diverse pleiotropic effects. Here, we address this problem using the concept of the joint distribution of fitness effects (JDFE), a local measurable property of the fitness landscape. We derive simple statistics of the JDFE that predict the expected slope, variance and covariance of non-home fitness trajectories. We estimate these statistics from published data from the *Escherichia coli* knock-out collection in the presence of antibiotics. We find that, for some drug pairs, the average trend towards collateral sensitivity may be masked by large uncertainty, even in the absence of epistasis. We provide simple theoretically grounded guidelines for designing robust sequential drug protocols.

Introduction

As a population adapts to one environment, it might concomitantly gain or lose fitness in other conditions. Such by-product ("pleiotropic") fitness gains and losses contribute to many eco-evolutionary processes. For example, pleiotropic fitness gains, also known as "buttressing pleiotropy", are in part responsible for the spread of invasive species and the expansion of virus host ranges (Lee, 2002; Lahti et al., 2009; Duffy et al., 2006; Bedhomme et al., 2015). Similarly, trade-offs between fitness in different environments in part determine the distribution of species across geographical regions or niches within the same habitat (Reusch and Woody, 2007; Friberg et al., 2008). Despite widespread observations of pleiotropy in nature (Futuyma and Moreno, 1988; Anderson et al., 2011; Forister et al., 2012; Chiang et al., 2013) and in the lab (reviewed in Andersson and Hughes, 2010; Bono et al., 2017; Elena, 2017)), some basic population genetic questions about the pleiotropic consequences of adaptation remain unresolved. What evolutionary parameters control whether a population adapting to one ("home") environment gains or loses fitness in another ("non-home") condition? What is the expected rate of such pleiotropic fitness changes? And what is the uncertainty around this expectation?

From the practical perspective, one of the most important implications of pleiotropy is collateral sensitivity and resistance in bacteria and cancers (Pluchino et al., 2012; Hutchison, 1963; Jensen et al., 1997; Hall et al., 2009; Imamovic and Sommer, 2013; Pál et al., 2015; Lázár et al., 2018; Barbosa et al., 2017). When a population treated with one drug acquires resistance against it, it may concomitantly become resistant to some other drug and/or susceptible to a third drug. The former situation, called collateral resistance, is an instance of a pleiotropic fitness gain. The latter, called collateral sensitivity, is an instance of a pleiotropic fitness loss. In a clinical setting, one would like to avoid collateral resistance, whereas collateral sensitivity may be exploited to develop sequential drug treatments which could help mitigate the looming multidrug resistance crisis (Bonhoeffer et al., 1997; Masterton, 2005; Imamovic and Sommer, 2013; Pál et al., 2015).

Developing successful sequential drug treatments hinges on knowing which drugs select for collateral sensitivity against which other drugs. Currently, this information can only be obtained empirically by exposing a bacterial or cancer-cell population to a drug and observing the evolutionary outcome (Bergstrom et al., 2004; Roemhild et al., 2020; Jensen et al., 1997; Imamovic and Sommer, 2013; Lázár et al., 2018; Maltas and Wood, 2019). Unfortunately, different experiments often produce collateral sensitivity profiles that are inconsistent with each other (e.g., Imamovic and Sommer, 2013; Oz et al., 2014; Maltas and Wood, 2019). Some of the inconsistencies can be attributed to the fact that resistance mutations vary between bacterial strains, drug dosages, etc. (Mira et al., 2015; Das et al., 2020; Pinheiro et al., 2020; Card et al., 2020). However, these factors cannot explain the wide variation in the pleiotropic outcomes of adaptation that are observed in replicate populations in the same experiment (Oz et al., 2014; Maltas and Wood, 2019; Nichol et al., 2019). Nichol et al. (2019) recently suggested that certain types of epistasis could

contribute to such variation. More generally, pleiotropic outcomes may be highly variable simply due to the intrinsic randomness of the evolutionary process, even in the absence of epistasis (Jerison et al., 2020). Yet, it is unclear which evolutionary parameters we need to know to predict the expected pleiotropic outcome of evolution and the uncertainty around such expectation.

Classical theoretical work on pleiotropy has been done in the field of quantitative genetics (Lande and Arnold, 1983; Rose, 1982; Barton, 1990; Slatkin and Frank, 1990; Jones et al., 2003; Johnson and Barton, 2005). These models were developed to understand how polygenic phenotypes respond to selection, and pleiotropy in these models manifests itself as a correlated temporal change in multiple traits that affect fitness in a given selection environment. The population genetic question of how new strongly beneficial mutations accumulating in one environment affect the population's fitness in future environments lies beyond the scope of these models (but see (Otto, 2004)). Pleiotropic consequences of adaptation have been explored in various "fitness landscape" models (e.g. Connallon and Clark, 2015; Martin and Lenormand, 2015; Harmand et al., 2017; Wang and Dai, 2019; Maltas et al., 2019; Tikhonov et al., 2020). This approach helps us understand the relationship between the global structure of the landscape and the outcomes of evolution. However, these models are not designed to be predictive because the global structure of the fitness landscape is extremely difficult to estimate.

Here we take a different approach which is agnostic with respect to the global structure of the fitness landscape. Instead, we assume only the knowledge of the so-called joint distribution of fitness effects (JDFE), i.e., the probability that a new mutation has a certain pair of fitness effects in the home and non-home environments (Jerison et al., 2014; Martin and Lenormand, 2015; Bono et al., 2017). JDFE is a natural extension of the DFE, the distribution of fitness effects of new mutations in the home environment (King, 1972; Ohta, 1987; Orr, 2003; Rees and Bataillon, 2006; Eyre-Walker and Keightley, 2007; Martin and Lenormand, 2008; MacLean and Buckling, 2009; Levy et al., 2015). The JDFE is a local property of the fitness landscape which means that it can be measured using a variety of modern techniques (Qian et al., 2012; Hietpas et al., 2013; Van Opijnen et al., 2009; Levy et al., 2015; Blundell et al., 2019). Since the short-term evolution of a population is determined by the pool of beneficial mutations that are currently available to the population, the knowledge of the JDFE should be sufficient to predict population's fitness in the non-home environment (Jerison et al., 2014).

Modeling evolution using the DFE and the JDFE is justified by the fact that there are usually many mutations that can improve the fitness of an organism in the home environment. These adaptive mutations affect a variety of genetic targets (Lang et al., 2013; Tenaillon et al., 2012; Kryazhimskiy et al., 2014; Venkataram et al., 2016; Good et al., 2017; Blundell et al., 2019) and provide fitness benefits of various magnitudes (Rees and Bataillon, 2006; MacLean and Buckling, 2009; Khan et al., 2011; Chou et al., 2011; Levy et al., 2015; Venkataram et al., 2016) via diverse physiological mechanisms (Travisano and Lenski, 1996; Jerison et al., 2020; Pinheiro et al., 2020; Kinsler et al.,

2020). As a consequence, different mutations also have diverse pleiotropic effects on fitness in non-home environments (Lenski, 1988; Ostrowski et al., 2005; Qian et al., 2012; Hietpas et al., 2013; Rodríguez-Verdugo et al., 2014; Jerison et al., 2020; Kinsler et al., 2020; Card et al., 2020). Recent evidence suggests that even when adaptive mutations are concentrated in relatively few genetic targets, they still exhibit a large variety of pleiotropic effects (Kinsler et al., 2020). Thus, we can model this mutational diversity as a joint probability distribution that a new mutation provides a certain fitness effect in the home environment and a certain fitness effect in the non-home environment. This modeling approach naturally produces a distribution of pleiotropic outcomes of adaptation among replicate populations evolving even in identical conditions. It can also naturally incorporate fitness trade-offs and some forms of epistasis, as we describe below.

To understand analytically how the JDFE determines the statistics of pleiotropy in an evolving population, we model evolution in the strong selection weak mutation (SSWM) regime. Our theory reveals a small number of key pleiotropy statistics of the JDFE that determine whether a population evolving in a home environment will on average gain or lose fitness in a non-home condition, how fast these pleiotropic changes are expected to accumulate, the uncertainty around these expectations and the correlation between fitness changes in the home and non-home environments. We verify that these parameters remain informative even outside of the SSWM regime and in the presence of some types of epistasis. Then, to gain an insight into the evolution of collateral resistance and sensitivity, we estimate the pleiotropy statistics of the antibiotic resistance JDFEs among knock-out mutations in bacterium *Escherichia coli*. Finally, we use our theory to provide guidance for designing sequential drug protocols.

Results

JDFE determines the pleiotropic outcomes of adaptation

For any genotype g that finds itself in one ("home") environment and may in the future encounter another "non-home" environment, we define the JDFE as the probability density $\Phi_g(\Delta x, \Delta y)$ that a new mutation that arises in this genotype has the selection coefficient Δx in the home environment and the selection coefficient Δy in the non-home environment (Jerison et al., 2014). We measure fitness of a genotype by its malthusian parameter (Crow and Kimura, 1972). So, if the home and non-home fitness of genotype g are x and y, respectively, and if this genotype acquires a mutation with selection coefficients Δx and Δy, its fitness becomes $x + \Delta x$ and $y + \Delta y$. This definition of the JDFE can of course be naturally extended to multiple non-home environments. In principle, the JDFE can vary from one genotype to another. However, to develop a basic intuition for how the JDFE determines pleiotropic outcomes, we initially assume that all genotypes have the same JDFE. We later explore how epistasis could affect our conclusions.

The JDFE is a complex object. So, we first asked whether some simple and intuitive summary statistics of the JDFE may be sufficient to predict the dynamics of the non-home fitness of a population which is adapting in the home environment. Intuitively, if there is a trade-off between home and non-home fitness, non-home fitness should decline; if the opposite is true, non-home fitness should increase. Canonically, a trade-off occurs when any mutation that improves fitness in one environment decreases it in the other environment and vice versa (Roff and Fairbairn, 2007). Genotypes that experience such "hard" trade-offs are at the Pareto front (Shoval et al., 2012; Li et al., 2019). For genotypes that are not at the Pareto front, some mutations that are beneficial in the home environment may be beneficial in the non-home environment and others may be deleterious. In this more general case, trade-offs are commonly quantified by the degree of negative correlation between the effects of mutations on fitness in the two environments (Roff and Fairbairn, 2007; Tikhonov et al., 2020). Thus, we might expect that evolution on negatively correlated JDFEs would lead to pleiotropic fitness losses and evolution on positively correlated JDFEs would lead to pleiotropic fitness gains.

To test this intuition, we generated a family of Gaussian JDFEs that varied, among other things, by their correlation structure (Figure 1; Materials and Methods). We then simulated the evolution of an asexual population on these JDFEs using a standard Wright-Fisher model (Materials and Methods) and tested whether the trade-off strength, measured by the JDFE's correlation coefficient, predicts the dynamics of non-home fitness. Figure 1 shows that our naive expectation is incorrect. Positively correlated JDFEs sometimes lead to pleiotropic fitness losses (Figure 1D,I), and negatively correlated JDFEs sometimes lead to pleiotropic fitness gains (Figure 1B,G). Even if we calculate the correlation coefficient only among mutations that are beneficial in the home environment, the pleiotropic outcomes still do not always conform to the naive expectation, as the sign of the correlation remains the same as for the full JDFEs in all these examples.

There are other properties of the JDFE that we might expect to be predictive of the pleiotropic outcomes of adaptation. For example, among the JDFEs considered in Figure 1, it is apparent that those with similar relative probability weights in the first and fourth quadrants produce similar pleiotropic outcomes. However, simulations with other JDFE shapes show that even distributions that are similar according to this metric can also result in qualitatively different pleiotropic outcomes (Supplementary Figure S1).

Overall, this analysis shows that JDFEs with apparently similar shapes can produce qualitatively different trajectories of pleiotropic fitness changes (e.g., compare Figures 1A,F and 1B,G or Figures 1D,I and 1E,J). Conversely, JDFEs with apparently different shapes can result in rather similar pleiotropic outcomes (e.g., compare Figures 1B,G and 1E,J or Figures 1A,F and 1D,I). Thus, while the overall shape of the JDFE clearly determines the trajectory of pleiotropic fitness changes, it is not immediately obvious what features of its shape play the most important role, particularly if the JDFE is more complex than a multivariate Gaussian.

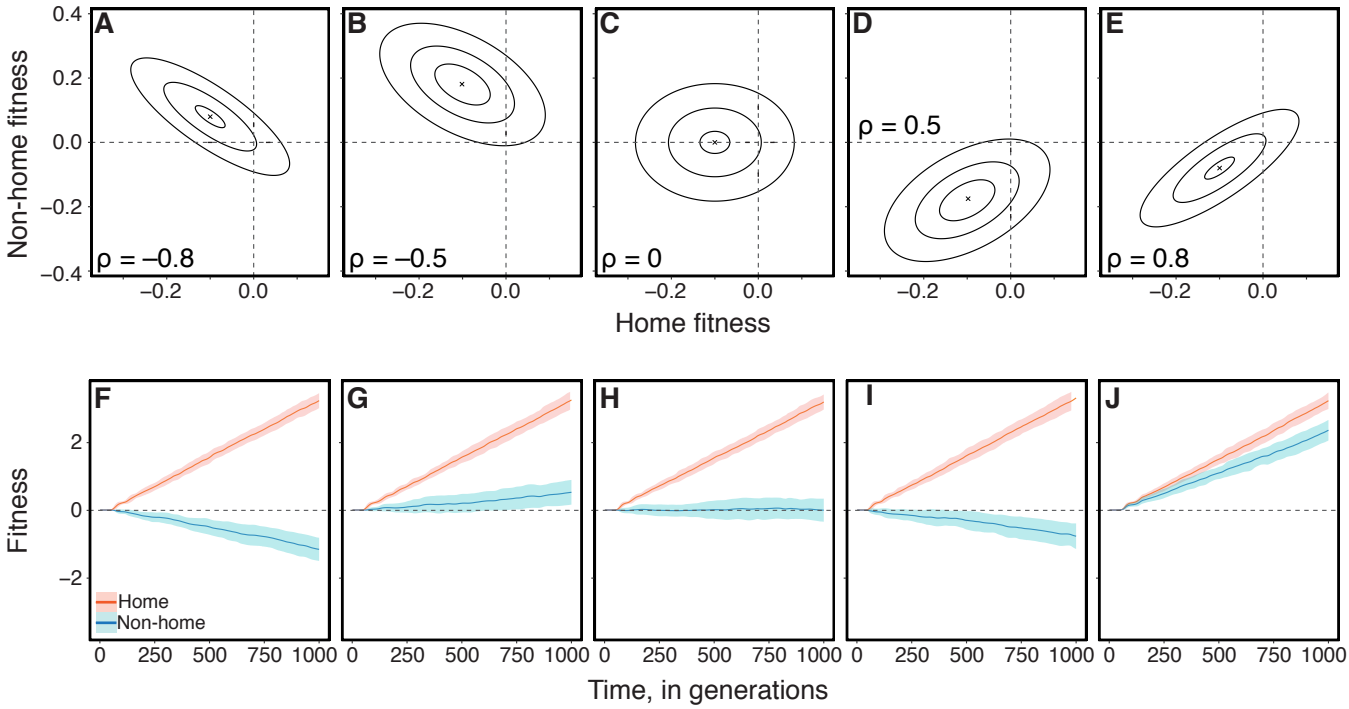

Figure 1. Gaussian JDFEs and the resulting fitness trajectories. A–E. Contour lines for five Gaussian JDFEs. "x" marks the mean. For all distributions, the standard deviation is 0.1 in both home- and non-home environments. The correlation coefficient ρ is shown in each panel **F–J.** Fitness trajectories for the JDFEs shown in the corresponding panels above. Ribbons show ± 1 standard deviation estimated from 100 replicate simulations. Population size $N = 10^6$, mutation rate $U = 10^{-4}$ ($U_b = 1.6 \times 10^{-5}$).

The population genetics of pleiotropy

To systematically investigate which properties of the JDFE determine the pleiotropic fitness changes in the non-home environment, we consider a population of size N that evolves on a JDFE in the "strong selection weak mutation" (SSWM) regime, also known as the "successional mutation" regime (Orr, 2000; Desai and Fisher, 2007; Kryazhimskiy et al., 2009; Good and Desai, 2015). We first analyze the evolution on JDFEs without epistasis and then consider how "global" epistasis affects our conclusions.

Non-epistatic JDFE. We consider an arbitrary JDFE without epistasis, that is a situation when all genotypes have the same JDFE $\Phi(\Delta x, \Delta y)$. We assume that mutations arise at rate U per individual per generation. In the SSWM limit, a mutation that arises in the population either instantaneously fixes or instantaneously dies out. Therefore, the population is essentially monomorphic at all times, such that at any time t we can characterize it by its current pair of fitness values (X_t, Y_t). If a new mutation with a pair of

selection coefficients $(\Delta x, \Delta y)$ arises in the population at time t, it fixes with probability $\pi(\Delta x) = \frac{1-e^{-2\Delta x}}{1-e^{-2N\Delta x}}$ (Kimura, 1962) in which case the population's fitness transitions to a new pair of values $(X_t + \Delta x, Y_t + \Delta y)$. If the mutation dies out, an event that occurs with probability $1-\pi(\Delta x)$, the population's fitness does not change. This model specifies a continuous-time two-dimensional Markov process.

In general, the dynamics of the probability density $p(x, y, t)$ of observing the random vector (X_t, Y_t) at values (x, y) are governed by an integro-differential forward Kolmogorov equation, which is difficult to solve (Materials and Methods). However, if most mutations that contribute to adaptation have small effects, these dynamics are well approximated by a diffusion equation which can be solved exactly (Materials and Methods). Then $p(x, y, t)$ is a normal distribution with mean vector

$$\boldsymbol{m}(t) = \begin{pmatrix} x_0 + r_1\, t \\ y_0 + r_2\, t \end{pmatrix} \tag{1}$$

and variance-covariance matrix

$$\boldsymbol{\sigma}^2(t) = \begin{pmatrix} D_{11}\, t & D_{12}\, t \\ D_{12}\, t & D_{22}\, t \end{pmatrix}, \tag{2}$$

where

$$r_1 = \int_{-\infty}^{\infty} d\eta \int_{0}^{\infty} d\xi\, \xi^2\, \Phi(\xi, \eta), \tag{3}$$

$$r_2 = \int_{-\infty}^{\infty} d\eta \int_{0}^{\infty} d\xi\, \eta\, \xi\, \Phi(\xi, \eta) \tag{4}$$

are the expected fitness effects in the home and non-home environments for a mutation fixed in the home environment, and D_{11}, D_{12} and D_{22} are the second moments of this distribution which are given by equations (9)–(11). Here, time is measured in units of $(2NU_b)^{-1}$ generations where $U_b = U \int_{-\infty}^{\infty} d\eta \int_{0}^{\infty} d\xi \Phi(\xi, \eta)$ is the total rate of mutations beneficial in the home environment, and x_0 and y_0 are the initial values of fitness of the population in the home and non-home environments.

Equations (1), (2) show that the distribution of population's fitness at time t in the non-home environment is entirely determined by three parameters, r_2, D_{22} and D_{12}, which we call the pleiotropy statistics of the JDFE. The expected rate of fitness change in the non-home environment depends on the pleiotropy statistic r_2, which we refer to as the expected pleiotropic effect. Thus, evolution on a JDFE with a positive r_2 is expected to result in pleiotropic fitness gains and evolution on a JDFE with a negative r_2 is expected to result in pleiotropic fitness losses. Equation (2) shows that the variance around this expectation is determined by the pleiotropy statistic D_{22}. Since both the expectation and the variance grow linearly with time (provided $r_2 \neq 0$), the change in the non-home fitness in any replicate population would eventually have the same sign as r_2, but the time scale

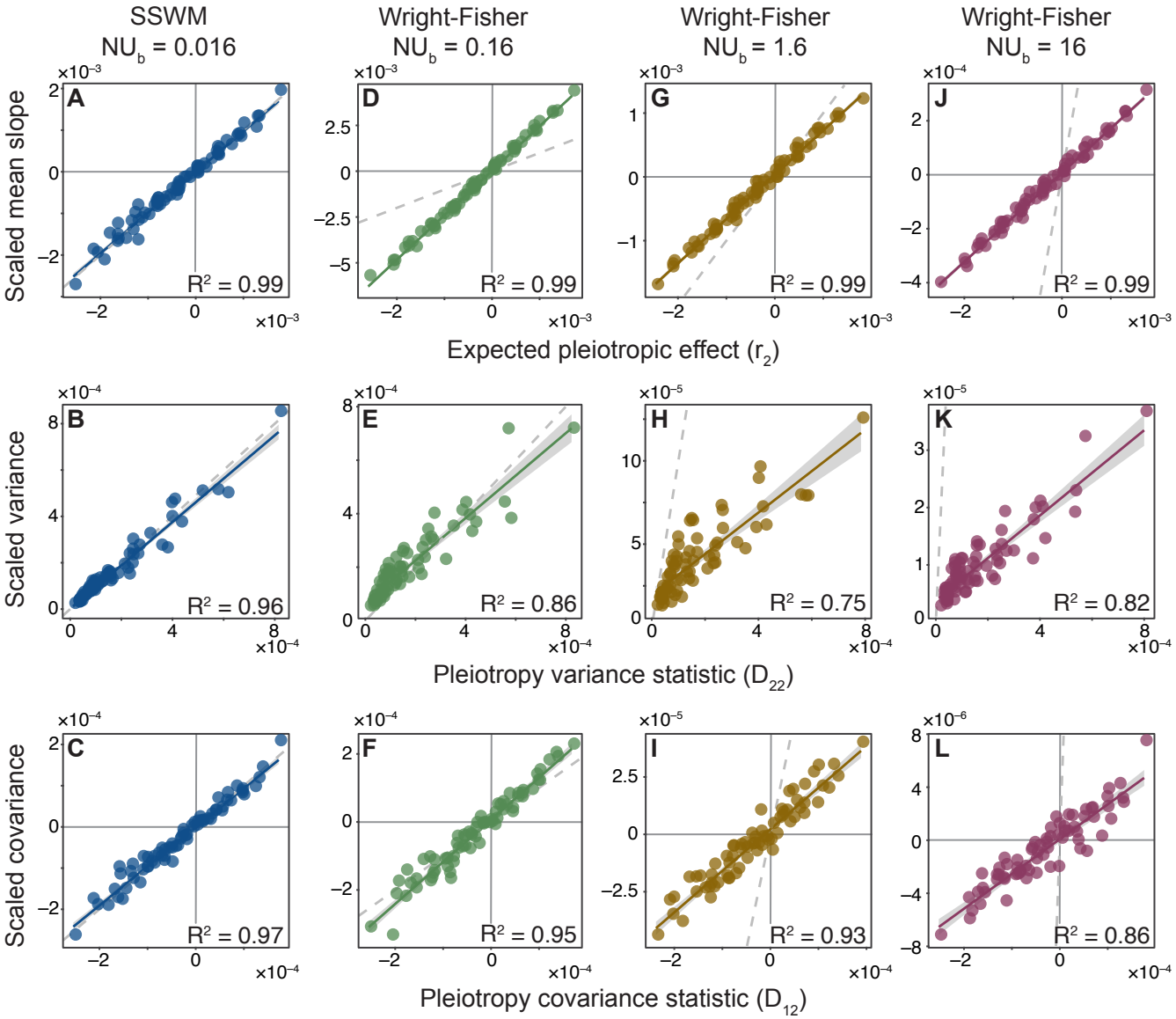

Figure 2. (Previous page). Pleiotropy statistics predict the properties of non-home fitness trajectories in simulations. Each point corresponds to an ensemble of simulations on one of 70 Gaussian JDFEs with the same population genetic parameters. (See Materials and Methods and Supplementary Table S1 for the JDFE parameters.) **A, D, G, J** (top row). Expected pleiotropic effect r_2 versus the slope of the mean non-home fitness (against time) observed in simulations. **B, E, H, K** (middle row). Pleiotropic statistic D_{22} versus the slope of the variance among non-home fitness (against time) observed in simulations. **C, F, I, L** (bottom row). Pleiotropic statistic D_{12} versus the slope of the covariance coefficient between home and non-home fitness (against time) observed in simulations. **A–C**. Evolution was simulated in the SSWM regime with the parameters indicated at the top, 500 replicates per data point (see Materials and Methods for details). **D–L**. Evolution was simulated using the full Wright-Fisher model with $N = 10^4$ and variable U as indicated at the top of each column, 100 replicates per data point (see Materials and Methods for details). In all panels, the values in the y-axis are the mean, variance covariance statistics obtained from simulations divided by $2NU_b$. Grey dashed line represents the identity (slope 1) line, and the solid line of the same color as the points is the linear regression for the displayed points (R^2 value is shown in each panel; $P < 2 \times 10^{-16}$ for all regressions).

of such convergence depends on the uncertainty parameter $c = \sqrt{D_{22}}/|r_2|$ (Materials and Methods). This observation has important practical implications, and we return to it in the Section "Evolution of collateral resistance and sensitivity in bacteria". In principle, knowing the pleiotropy statistics r_2 and D_{22} is sufficient to probabilistically predict the non-home fitness of the population at any time t. However, if its home fitness at time t is also known, this prediction can be further refined using the pleiotropy covariance statistic D_{12}.

We tested the validity of equations (1) and (2) by simulating evolution in the SSWM regime on 70 Gaussian JDFEs with various parameters (Materials and Methods) and found excellent agreement (Figure 2A–C). We next asked whether the three pleiotropy statistics, r_2, D_{22} and D_{12}, can predict the non-home fitness trajectories when the underlying evolutionary dynamics fall outside of the SSWM regime, i.e., when multiple beneficial mutations segregate in the population simultaneously (the "concurrent mutation" regime (Desai and Fisher, 2007; Good et al., 2012)). To this end, we simulated evolution on the same 70 JDFEs using the full Wright-Fisher model with a range of population genetic parameters that span the transition from the successional mutation regime to the concurrent mutation regime, for 1000 generations. We found that the rate of change in non-home fitness mean, variance and covariance remain highly correlated with the corresponding pleiotropy statistics (Figure 2). However, while in the SSWM regime the pleiotropy statistics are quantitative predictors, in the sense that the observed values fall on the diagonal in Figures 2A–C, outside of the SSWM regime they are only statistical predictors, in the sense that the observed values fall on a line but not the diagonal in Figures 2D–L. In other words, the dynamics of adaptation in the concurrent and suc-

cessional mutations regime are different. Nevertheless, the pleiotropy statistics reliably predict whether a population would gain or lose fitness in the non-home environment and allow us to rank environment pairs according to the rates and repeatability of these gains or losses.

JDFE with global epistasis. Our results so far were derived under the assumption that all genotypes have the same JDFE. In reality, JDFEs probably vary from one genotype to another, but how they vary is not yet known. Recently, researchers began to systematically probe how the effects of new individual mutations on fitness in one environment and their distribution (i.e., the DFE) vary among genotypes (Khan et al., 2011; Chou et al., 2011; Kryazhimskiy et al., 2014; Johnson et al., 2019; Wang et al., 2016; Aggeli et al., 2020). These studies suggest that the fitness effects of mutations available to a genotype and its overall DFE in a given environment depend primarily on the fitness of that genotype in that environment, a phenomenon referred to as "global epistasis" (Wiser et al., 2013; Kryazhimskiy et al., 2014; Reddy and Desai, 2020; Husain and Murugan, 2020). Thus, we next sought to understand how such epistasis might affect the pleiotropic outcomes of adaptation.

Global epistasis can be modeled in our framework by assuming that the JDFE of genotype g depends only the fitness of this genotype in the home and non-home environments, $x(g)$, $y(g)$, i.e. $\Phi_g(\Delta x, \Delta y) = \Phi_{x(g),y(g)}(\Delta x, \Delta y)$, which is a two-dimensional extension of the model considered in (Kryazhimskiy et al., 2009). Thus, in the SSWM regime, the population can still be fully described by its current pair of fitness values in the home and non-home environments (X_t, Y_t). The dynamics of the probability density $p(x, y, t)$ are governed by the same Kolmogorov equation as in the non-epistatic case, which can still be approximated by a diffusion equation (equation (8) in the Materials and Methods). However, while in the non-epistatic case the drift and diffusion coefficients of this equation, r_1, r_2, D_{11}, D_{12} and D_{22} are constants, in the presence of global epistasis, they become functions of x and y. Although this equation cannot be solved analytically in the general case, it can be solved numerically, provided that the functions $r_1(x, y)$, $r_2(x, y)$, $D_{11}(x, y)$, $D_{12}(x, y)$ and $D_{22}(x, y)$ are known. Thus, in principle, our theory can predict the trajectories of non-home fitness in the presence of global epistasis.

As in the non-epistatic case, it is a priori unclear whether our theory retains its predictive power in the concurrent mutations regime. To test it, we focus on one particular model of a JDFE with global epistasis. In this model, we neglect mutations that are deleterious in the home environment and consider the home-environment DFE to be an exponential distribution with the mean that linearly decays with the genotype's home fitness (see Figure 3A–D and Materials and Methods). The non-home-environment DFE is a Gaussian distribution with mean and variance that do not depend on the genotype's current fitness. We allow for an arbitrary correlation between home and non-home fitness. This form of the JDFE is consistent with our current understanding of the structure of global epistasis (Kryazhimskiy et al., 2014; Johnson et al., 2019; Lukačišinová et al., 2020).

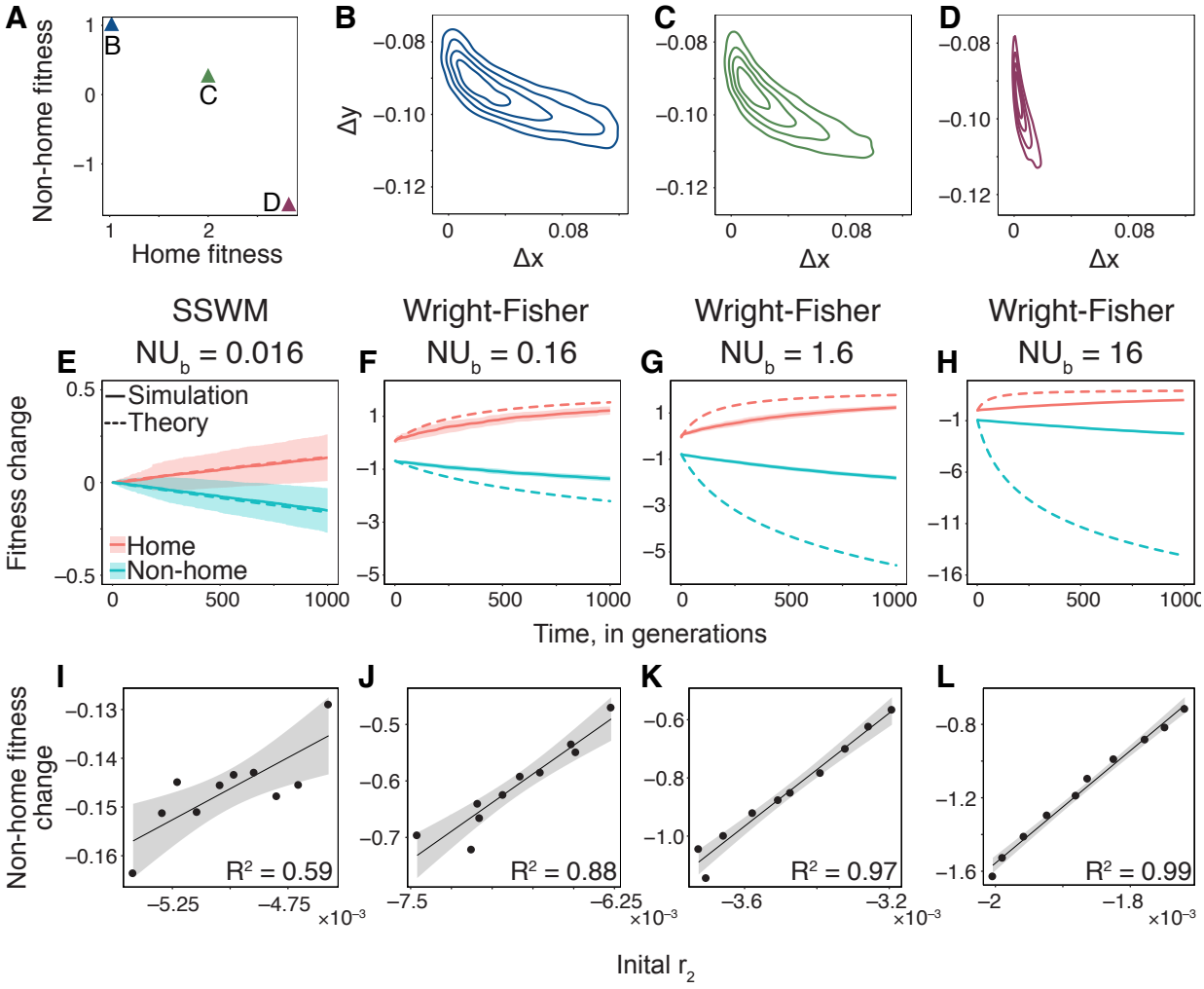

Figure 3. Evolution on a JDFE with global diminishing returns epistasis. A–D. JDFE with global epistasis where genotype's JDFE depends on its fitness (see text and Materials and Methods for details). Panel A shows three pairs of home- (x) and non-home (y) fitness for which the JDFEs are shown in panels B,C,D, as indicated. Δx and Δy are the fitness effects of a new mutation in the home- and non-home environments, respectively. **E–H.** Trajectories of mean change in home and non-home fitness. Simulations were performed as described in Materials and Methods , with 100 replicates per panel. To improve visual clarity, simulations in different panels were performed on JDFEs with different values of parameter γ (see Materials and Methods for details). Ribbons show ± 1 standard deviation across replicate simulations. **I–L.** Expected pleiotropic effect r_2 evaluated at the initial time point versus the mean change in population's non-home fitness after 1,000 generations in the corresponding simulations shown above in panels E–H. Variation in r_2 was generated by altering the correlation of the JDFEs (see Materials and Methods). Solid line is linear regression, $P < 0.006$ for all panels. Grey ribbons represent standard error of the regression.

In this model, it is possible to obtain analytical expressions for the expected fitness trajectories of the population $\langle X_t \rangle$, $\langle Y_t \rangle$ in the home and non-home environments (see Materials and Methods). As expected, our theory quantitatively predicts the fitness trajectories obtained in stochastic SSWM simulations (Figure 3E). The trajectories simulated with the full Wright-Fisher model in the concurrent mutation regime deviate substantially from our predictions. However, the sign of the function r_2 still reliably predicts the expected direction of non-home fitness change (Figure 3F–H). Moreover, the pleiotropy statistic $r_2(x_0, y_0)$, i.e., r_2 evaluated for the ancestral genotype, is a good predictor of the relative magnitude of the change in non-home fitness (Figure 3I–L). We conclude that our theory remains useful even in the presence of some forms of epistasis.

Evolution of collateral resistance and sensitivity in bacteria

We next sought to apply our theoretical results to understand how bacteria adapting to one antibiotic develop collateral resistance and/or sensitivity to other antibiotics. To do so, we need to know the full bacterial JDFEs in the presence of antibiotics. Estimating such full JDFEs is difficult because it requires large samples of mutations that have a reasonable chance of fixing in the home environment. Because the techniques for obtaining such samples became only recently available (Levy et al., 2015; Venkataram et al., 2016), full bacterial JDFEs are not yet available. To circumvent this problem, we investigate the pleiotropic consequences of evolution on the joint distributions of fitness effects of knock-out mutations (koJDFEs). In contrast to full JDFEs, koJDFEs can be readily estimated from fitness measurements in knock-out collections (Qian et al., 2012; Chevereau et al., 2015) or from Tn-Seq experiments in various bacteria (Van Opijnen et al., 2009; Wetmore et al., 2015; Morin et al., 2018). We do not expect the koJDFEs to be identical to the corresponding full JDFEs. However, since knock-outs are a subset of all mutations, koJDFEs give us a lower bound on the breadth of fitness effects of new mutations. Furthermore, because loss-of-function mutations play an important role in adaptive evolution in microbes, including the evolution of antibiotic resistance (Kohanski et al., 2007; Schurek et al., 2008; Török et al., 2012; Hottes et al., 2013; D'Souza et al., 2014), the koJDFEs may be reasonable zeroth order approximations for the full JDFE. Supporting this conjecture, Chevereau et al. (2015) showed that the dynamics of short-term adaptive evolution in the presence of an antibiotic can be predicted using knock-out data.

We obtained the growth rate measurements of 3883 *E. coli* gene knockout mutants in the presence of six different antibiotics from the study by Chevereau et al. (2015). From these data, we could in principle estimate the koJDFEs in 30 ordered drug pairs. However, to justify using the JDFE framework, we first need to establish whether there is a sufficient number of beneficial knock-out mutations in the presence of each drug. In four out of six antibiotics, we found that between 24 (0.62 %) and 329 (8.47 %) of knock-out mutations are adaptive at the false discovery rate (FDR) of $\sim 25\%$ (Figure 4; Supplementary Table S2). In the remaining two drugs, chloramphenicol and trimethoprim, we could

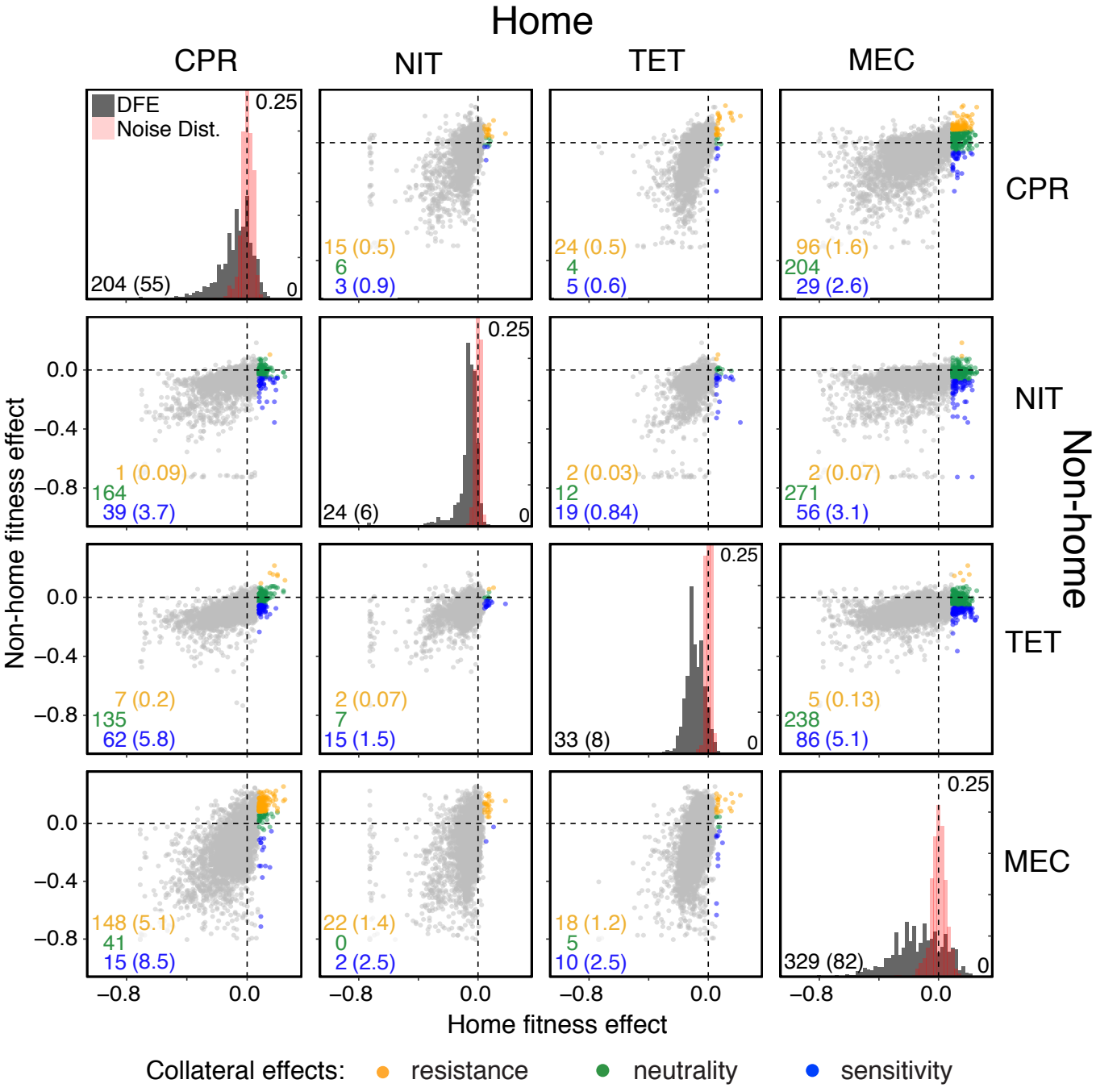

Figure 4. (Previous page) Empirical koJDFEs for *E. coli* in the presence of four antibiotics, based on data obtained by Chevereau et al. (2015). Panels on the diagonal show the distributions of fitness effects (DFEs) of knock-out mutations in the presence of corresponding antibiotics (equivalent to Figure 1C in Chevereau et al. (2015)). The estimated measurement noise distributions are shown in red (see Materials and Methods for details). Note that the noise distributions are vertically cut-off for visual convenience. The number of identified beneficial mutations (i.e., resistance mutations) and the expected number of false positives (in parenthesis) are shown in the bottom left corner. Off-diagonal panels show the koJDFEs. Each point corresponds to an individual knock-out mutation. Identified resistance mutations are colored according to their collateral effects, as indicated in the legend. The numbers of mutations of each type are indicated in the corresponding color in the bottom left corner of each panel. The expected numbers of false positives are shown in parenthesis.

not reliably discriminate between adaptive mutations and measurement noise (Materials and Methods), so we excluded these antibiotics from further analysis. Plotting the fitness effect of each knock-out mutation in one drug against its effect in another drug, we find that, for all 12 ordered drug pairs, there exist mutations in all four quadrants of this plane (Figure 4, Supplementary Table S2). Thus, even when we consider only knock-out mutations, no drug pair exhibits hard trade-offs, i.e., a fitness gain in the presence of any drug can come either with a pleiotropic gain or a pleiotropic loss of fitness in the presence of another drug. We conclude that the JDFE framework is suitable for modeling the evolution of collateral resistance/sensitivity.

For each of the 12 koJDFEs, we computed the pleiotropy statistics r_2, D_{22}, D_{12} (Figure 5A, B; Supplementary Table S3) using mutations with significant beneficial effects in the home environment. Our results remain robust with respect to changes in the FDR (see Supplementary Figure S3 and Supplementary Table S4). Because some of the koJDFEs are markedly non-Gaussian, we sought to verify that the pleiotropy statistics still accurately capture how populations evolve on these more realistic JDFEs. To this end, we simulated evolution on all 12 koJDFEs using the Wright-Fisher model with $N = 10^4$ and mutation rate $U = 10^{-2}$ ($NU = 100$), taking care to account for the uncertainty in our estimates of these koJDFEs caused by measurement noise (Materials and Methods). Our simulations confirm that the expected non-home fitness gains, their variances and covariances are still predicted by the pleiotropy statistics of the underlying koJDFEs (Supplementary Figure S2).

To understand what patterns of collateral resistance and sensitivity we would expect to observe on these koJDFEs, we examined the structure of the matrices of the pleiotropic parameters. We found that the expected pleiotropic effect r_2 varies widely among drug pairs. One striking feature of the r_2 matrix is its asymmetry, i.e., the fact that, for many drug pairs, the order of the drugs affects the sign of the expected pleiotropic effect (Figure 5A). As discussed above, this sign determines whether the population evolving in the presence of the first drug eventually acquires collateral resistance or collateral sensitivity

to the second drug. For example, if ciproflaxin (CPR) is used first (home environment) and nitrofurantoin (NIT) is used second (non-home environment), the expected pleiotropic effect is negative, which indicates that acquisition of resistance against CPR will eventually lead to collateral sensitivity to NIT. If these drugs are applied in the reverse order, the expected pleiotropic effect is positive, which indicates that the acquisition of resistance against NIT will eventually lead to collateral resistance against CPR. In fact, NIT is in general a poor choice for the first drug in a sequential treatment as it is expected to generate collateral resistance against at least two drugs (MEC and CPR) and only weak collateral sensitivity against TET (Figure 5A). On the other hand, NIT may be a good candidate for the second drug in a sequential treatment since multiple other drugs are expected to produce collateral sensitivity against it (Figure 5A).

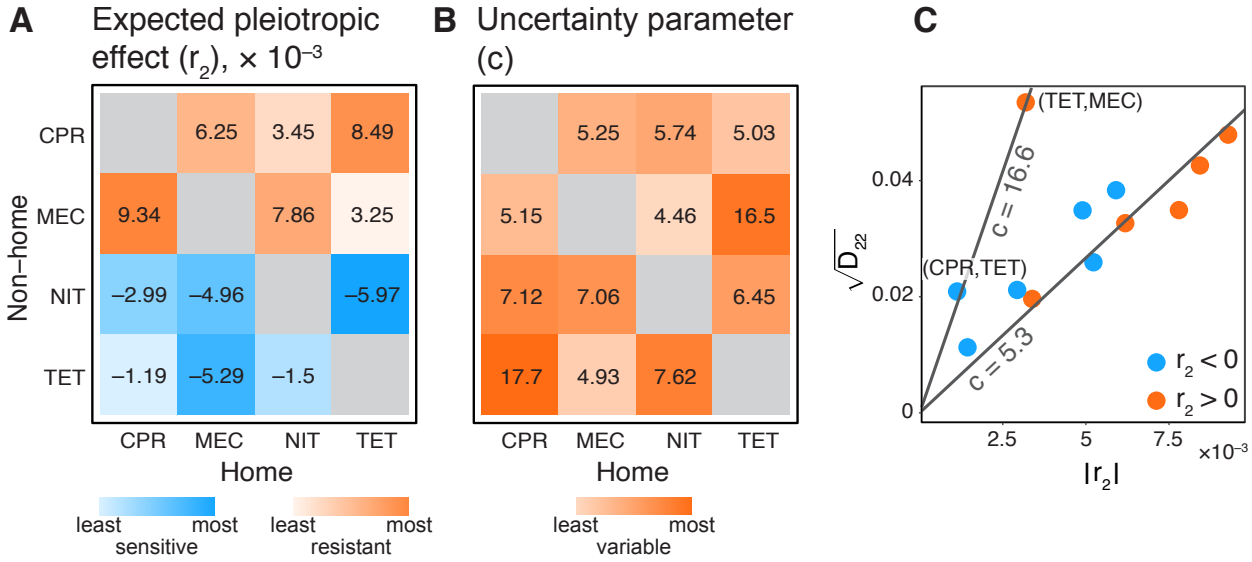

Figure 5. Pleiotropic parameters of koJDFEs in *E. coli* in the presence of antibiotics. **A.** The matrix of expected pleiotropic effects r_2, colored by rank order. **B.** The matrix of uncertainty parameters c, colored by rank order. **C.** Scaling of the pleiotropy statistics. Each point is an ordered drug pair. Points are colored by the sign of the r_2 value. Parameters are estimated from knock-out mutations that are beneficial in the home environment at $\sim 25\%$ FDR (see Figure 4 and text).

Even though some drugs are expected to lead to collateral sensitivity against some other drugs eventually, the actual collateral resistance/sensitivity state of any individual population after a treatment with the first drug might be the opposite of this expectation (Maltas and Wood, 2019; Nichol et al., 2019). For example, by the time that the average population evolving in the presence of NIT loses 40% percent of fitness in TET (i.e., becomes collaterally sensitive to TET), 17% of individual populations will have acquired collateral resistance against TET. Our theory shows that such departures from the expectation become less likely with longer treatments, and their probability depends on the

uncertainty parameter c: the larger c, the more likely is a departure from expectation. Thus, a successful sequential drug treatment protocol needs to satisfy two criteria. First, the expected pleiotropic effects (r_2) for all sequential drug pairs should be negative and as large by absolute value as possible. This will ensure that the evolution in the presence of the preceding drug will on average induce stronger collateral sensitivity to the following drug. Second, all values of the uncertainty parameter c should be as small as possible. This will ensure that any individual population adapting to the preceding drug rapidly achieves sensitivity against the following drug.

Is it possible to satisfy both of these criteria? To answer this question, we examined how the pleiotropy statistics co-vary among drug pairs. We find that the square root of the variance parameter D_{22} and the expected pleiotropic effect r_2 linearly co-vary for most drug pairs, so that the uncertainty parameter c is concentrated around 5 (Figure 5C). Two pairs, (TET,MEC), (CPR,TET) have a much larger uncertainty parameter ~ 17. The approximately linear relationship between $\sqrt{D_{22}}$ and r_2 is preserved if relax our FDR cutoff (Supplementary Figure S3). These results suggest that, as long as drug pair with abnormally high uncertainty parameter c are avoided, selection of drugs for sequential treatment based solely on the expected effect r_2 will produce surprisingly robust sequential protocols. However, it is important to keep in mind that this conclusion is based on limited data and its generality needs to be further scrutinized.

In summary, it is natural to model the evolution of collateral resistance and sensitivity within the JDFE framework. Although bacterial JDFEs in the presence of antibiotics are currently unknown, our analysis of the knock-out data suggests that they have a wide variety of shapes. Our theory provides a principled way to select drugs for designing robust sequential drug treatments based on their pleiotropy statistics.

Discussion

We have developed a basic theory which describes how a population evolving in a home environment concomitantly gains or loses fitness in a non-home environment, how fast and with what probability. The central concept of our theory is the joint distribution of fitness effects of mutations (JDFE), a measurable local property of the fitness landscape. The idea behind the JDFE is that adaptation can be driven by many beneficial mutations with diverse pleiotropic effects. In other words, fitness gains in the home environment do not inevitably lead to either fitness losses (hard trade-offs) or fitness gains (hard buttressing pleiotropy) in the non-home environment, although they may have a tendency to do so.

We have shown that a small number of intuitively interpretable parameters of the JDFE can be used to predict the pleiotropic outcomes of evolution. Specifically, the expected pleiotropic effect (parameter r_2) predicts the average rate at which fitness in the non-home environment will be gained (if $r_2 > 0$) or lost (if $r_2 < 0$). The pleiotropy variance parameter D_{22} predicts how strongly the non-home fitness in any individual

population would deviate from the expectation. Regardless of D_{22}, as time goes on, any individual population adapting to the home environment will eventually gain fitness in the non-home environment (if $r_2 > 0$) or lose it (if $r_2 < 0$). In the absence of epistasis, the time scale of such convergence depends on the uncertainty parameter $c = \sqrt{D_{22}}/|r_2|$. Finally, the covariance parameter D_{12} allows us to predict the non-home fitness of the population if we know its home fitness. Using simulations, we have shown that these parameters statistically predict the outcomes of evolution even outside of the SSWM regime where they were derived.

Most of our results were obtained for constant JDFEs, i.e., in the absence of epistasis. The predictive power of such non-epistatic theory is expected to decline with time, for two reasons. First, as the population accumulates mutations that are beneficial in the home environment, these mutations are removed from the beneficial part of the JDFE thereby changing its structure. The second reason is epistasis, i.e., the fact that different genotypes probably have different JDFEs. Even if each individual mutation alters the effects of other mutations only slightly, these small changes will accumulate and the structure of the JDFE will eventually change. We have examined how one particularly simple type of epistasis—diminishing returns—could affect the evolutionary dynamics of pleiotropy. Our results show that the r_2 parameter remains correlated with non-home fitness in the presence of this type of epistasis. Empirically measuring how JDFEs vary across genotypes and theoretically understanding how such variation would affect the evolution of pleiotropic outcomes are important open problems.

We applied our theory to understand the evolution of collateral resistance and sensitivity in bacteria. We used previously published data to estimate the JDFE of knock-out mutations (koJDFE) in *E. coli* in the presence of several commonly used antibiotics. We found that many knock-outs significantly improve fitness in the presence of single drugs and that these mutations have diverse beneficial and deleterious pleiotropic effects in the presence of other drugs. In other words, we did not find evidence for hard physiological trade-offs or buttressing pleiotropy, even among knock-out mutations. Since knock-outs are a subset of all mutations, the diversity of pleiotropic effects among all mutations must be even greater. Thus, modeling antibiotic resistance within the JDFE framework is appropriate.

Based on our theory, we proposed two simple rules for designing robust sequential drug treatments. First, the expected pleiotropic effect (that is, the parameter r_2 of the JDFE) for all sequential drug pairs in the treatment should be negative and maximal by magnitude. Second, the uncertainty parameter c of the JDFE for all sequential drug pairs should be minimal. The first rule ensures that resistance to the previous drug in the sequence on average leads to collateral sensitivity to the next drug. The second rule ensures that the deviations from this average are as small as possible.

Examining the pleiotropy statistics of the koJDFEs, we found that the expected pleiotropic effect r_2 varies substantially among different drug pairs but the uncertainty parameter c is surprisingly similar for most drug pairs, with a few exceptions. Thus,

our analysis suggests that selecting drugs for a sequential treatment based only on the expected pleiotropic effect may not be as bad as one might have expected a priori. It is however important to keep in mind the limitations of our analysis. Specifically, errors in the measurements of growth rate were quite large in this data set, preventing us from calling mutations with small fitness benefits and defects which nevertheless could be important for evolution. Improved fitness estimates could lead to changes in the estimates of pleiotropic parameters. Another caveat is that our estimates are based on knock-out mutations. Full JDFEs could differ substantially from the koJDFEs that we examined here. Finally, the availability and the type of resistance mutations depend on drug concentrations, other environmental conditions and on the bacterial species and strain (Lindsey et al., 2013; Das et al., 2020; Pinheiro et al., 2020; Card et al., 2020). All these factors could significantly affect the JDFE shape. These caveats notwithstanding, our observations provide the first glimpse of how bacterial JDFEs in the presence of antibiotics might look like.

Previous studies of collateral antibiotic resistance/sensitivity have been retrospective and phenomenological, in the sense that we could learn whether and to what degree any particular population would evolve collateral resistance or sensitivity only after observing its evolution. Ascertaining robustness of such results is very challenging with respect to any kind of perturbations, including variations in the population-genetic parameters, such as population size or mutation rate. In contrast, JDFE does not depend on these parameters; it is a property of the genotype and the environment. Thus, although the JDFE must still be empirically measured, our approach accounts for the population genetics of adaptation. Thus, JDFE-based evolutionary predictions of collateral resistance and sensitivity should be more robust than purely phenomenological ones.

Perhaps the most important practical implication of our results is that, because resistance mutations have a wide range of collateral effects, it is essential to consider the repeatability of collateral resistance/sensitivity evolution in designing sequential drug protocols. In other words, our results support the conclusion of Nichol et al. (2019) et al that experimental studies of collateral resistance/sensitivity should be carried out with sufficient replication, so that the distribution of collateral outcomes can be accurately estimated, at least for the most promising drug pairs.

Materials and Methods

Theory

We assume that an asexual population evolves according the Wright-Fisher model in the strong selection weak mutation (SSWM) limit (Orr, 2000; Kryazhimskiy et al., 2009; Good and Desai, 2015), also known as the "successional mutations" regime (Desai and Fisher, 2007). In this regime, the population remains monomorphic until the arrival of a new mutation that is destined to fix. The waiting time for such new mutation is assumed to

be much longer than the time it takes for the mutation to fix, i.e., fixation happens almost instantaneously on this time scale, after which point the population is again monomorphic. If the per genome per generation rate of beneficial mutations is U_b, their typical effect is s and the population size is N, the SSWM approximation holds when $NU_b \ll 1/\ln(Ns)$ (Desai and Fisher, 2007).

We describe our population by a two-dimensional vector of random variables (X_t, Y_t), where X_t and Y_t are the population's fitness (growth rate or the Malthusian parameter) in the home and non-home environments at generation t, respectively. We assume that the fitness vector of the population at the initial time point is known and is (x_0, y_0). We are interested in characterizing the joint probability density $p(x, y, t)\, dx\, dy = \Pr\{X_t \in [x, x + dx), Y_t \in [y, y + dy)\}$.

Constant JDFE

We first consider the simple case when all genotypes have the same JDFE $\Phi(\Delta x, \Delta y)$. In the exponential growth model, the selection coefficient of a mutation is the difference between the mutant and the ancestor growth rates in the home environment, i.e., Δx. The probability of fixation of the mutant is given by Kimura's formula, which we approximate by $2\Delta x$ for $\Delta x > 0$ and zero otherwise (Crow and Kimura, 1972).

If the total rate of mutations (per genome per generation) is U, the rate of mutations beneficial in the home environment is given by U_b, that is $U_b = U \int_{-\infty}^{\infty} d\eta \int_0^{\infty} d\xi\ \Phi(\xi, \eta)$. Then, in the SSWM limit, our population is described by a two-dimensional continuous-time continuous-space Markov chain with the transition rate from state (x, y) to state (x', y') given by

$$Q(x', y'|x, y) = \begin{cases} 2NU_b\,(x' - x)\,\Phi(x' - x, y' - y) & \text{if } x' > x, \\ 0 & \text{otherwise.} \end{cases}$$

or, after rescaling time by $2NU_b$,

$$Q(x', y'|x, y) = \begin{cases} (x' - x)\,\Phi(x' - x, y' - y) & \text{if } x' > x, \\ 0 & \text{otherwise.} \end{cases} \tag{5}$$

The probability distribution $p(x, y, t)$ satisfies the integro-differential forward Kolmogorov equation (Van Kampen, 1992)

$$\begin{aligned} &\frac{\partial p}{\partial t}(x, y, t) \\ &= \int_{-\infty}^{\infty} d\eta \int_{-\infty}^{\infty} d\xi \Big(p(\xi, \eta, t)\, Q(x, y|\xi, \eta) - p(x, y, t)\, Q(\xi, \eta|x, y) \Big) \end{aligned} \tag{6}$$

with the initial condition

$$p(x, y, 0) = \delta(x - x_0)\,\delta(y - y_0). \tag{7}$$

When beneficial mutations with large effects are sufficiently rare, equation (6) can be approximated by the Fokker-Planck equation (Van Kampen, 1992)

$$\frac{\partial p}{\partial t} = -r_1 \frac{\partial p}{\partial x} - r_2 \frac{\partial p}{\partial y} + \frac{D_{11}}{2} \frac{\partial^2 p}{\partial x^2} + D_{12} \frac{\partial^2 p}{\partial x \partial y} + \frac{D_{22}}{2} \frac{\partial^2 p}{\partial y^2}, \tag{8}$$

where r_1 and r_2 are given by equations (3), (4) and

$$D_{11} = \int_{-\infty}^{\infty} d\eta \int_{0}^{\infty} d\xi \, \xi^3 \, \Phi(\xi, \eta), \tag{9}$$

$$D_{12} = \int_{-\infty}^{\infty} d\eta \int_{0}^{\infty} d\xi \, \eta \, \xi^2 \, \Phi(\xi, \eta), \tag{10}$$

$$D_{22} = \int_{-\infty}^{\infty} d\eta \int_{0}^{\infty} d\xi \, \eta^2 \, \xi \, \Phi(\xi, \eta) \tag{11}$$

are the second moments of the distribution of the fitness effects of mutations fixed in the home environment.

The solution to equation (8) with the initial condition (7) is a multi-variate normal distribution with the mean vector $\boldsymbol{m}(t)$ and the variance-covariance matrix $\boldsymbol{\sigma}^2(t)$ given by equations (1), (2). Since both the mean and the variance of Y_t scale linearly with time, the bulk of the non-home fitness distribution will eventually shift above y_0 (if $r_2 > 0$) or below y_0 (if $r_2 < 0$). In fact, it is easy to see that, for any positive number Z, the mean of this distribution will be at least Z standard deviations above y_0 (if $r_2 > 0$) or below y_0 (if $r_2 < 0$) after time $t_Z = Z^2 \, D_{22}/r_2^2$. In other words, the time scale of convergence of the non-home fitness effect to the expectation is controlled by the parameter $c = \sqrt{D_{22}}/|r_2|$.

JDFE with global epistasis

It is straightforward to incorporate global epistasis into a Gaussian JDFE model, but analytical calculations become cumbersome. To simplify theses calculations, we consider the following convenient JDFE shape.

$$\Phi(\xi, \eta) = \frac{1}{\mu_1 \sqrt{2\pi\sigma^2 \, (1-\rho^2)}} \exp\left(-\frac{\xi}{\mu_1} - \frac{\left(\eta - \mu_2 - \frac{\rho\,\sigma}{\mu_1}(\xi - \mu_1)\right)^2}{2\,\sigma^2 \, (1-\rho^2)} \right),$$
$$\xi \in \mathbb{R}_+, \; \eta \in \mathbb{R} \tag{12}$$

Note that this distribution is defined only for $\xi \geq 0$, i.e., we assume that mutations deleterious in the home environment never fix.

According to equation (12), the DFE in the home environment is an exponential distribution $p_1(\xi)$ with mean μ_1, and the conditional DFE $p_2(\eta|\xi)$ in the non-home environment,

given that the effect of mutation the home in environment is ξ, is a normal distribution with mean and variance

$$\begin{aligned} \mu_2'(\xi) &= \mu_2 + \frac{\rho\,\sigma}{\mu_1}(\xi - \mu_1), \\ (\sigma')^2 &= \sigma^2\,\left(1-\rho^2\right). \end{aligned}$$

Thus, distribution (12) has four parameters μ_1, μ_2, σ^2 and ρ. It is easy to check that μ_1 and μ_2 are the expected effects of a random mutation in the home and non-home environments, respectively; σ^2 is the variance of the distribution of effects of mutations on fitness in the non-home environment; ρ is the correlation coefficient between the effects of mutations in the home and non-home environments.

Using the fact that

$$\langle \xi^n \rangle = n!\,\mu_1^n,$$

we obtain

$$\begin{aligned} r_1 &= \int_0^\infty \xi^2\,p_1(\xi)\,d\xi \int_{\mathbb{R}} p_2(\eta|\xi)\,d\eta = \langle \xi^2 \rangle = 2\mu_1^2, \\ r_2 &= \int_0^\infty \xi\,p_1(\xi)\,d\xi \int_{\mathbb{R}} \eta\,p_2(\eta|\xi)\,d\eta = \langle \xi\,\mu_2'(\xi) \rangle = \mu_1\,(\mu_2 + \rho\,\sigma) \end{aligned}$$

and

$$\begin{aligned} D_{11} &= \int_0^\infty \xi^3\,p_1(\xi)\,d\xi \int_{\mathbb{R}} p_2(\eta|\xi)\,d\eta = \langle \xi^3 \rangle = 6\mu_1^3, \\ D_{12} &= \int_0^\infty \xi^2\,p_1(\xi)\,d\xi \int_{\mathbb{R}} \eta\,p_2(\eta|\xi)\,d\eta = \langle \xi^2\,\mu_2'(\xi) \rangle \\ &= 2\mu_1^2\,(\mu_2 + 2\,\rho\,\sigma)\,, \\ D_{22} &= \int_0^\infty \xi\,p_1(\xi)\,d\xi \int_{\mathbb{R}} \eta^2\,p_2(\eta|\xi)\,d\eta = \left\langle \xi\,\left((\sigma')^2 + (\mu_2'(\xi))^2\right) \right\rangle \\ &= \mu_1\,\left[\sigma^2 + \mu_2^2 + 2\rho\,\sigma + 2\rho^2\,\sigma^2\right]. \end{aligned}$$

Next, we model global diminishing returns epistasis by assuming that the mean of the DFE in the home environment μ_1 declines with the fitness of the genotype in the home environment x (Kryazhimskiy et al., 2014; Aggeli et al., 2020), i.e.,

$$\mu_1 = \gamma_1\,(x_{\max} - x)\,. \tag{13}$$

We will assume that the mean μ_2, variance σ^2 and the correlation coefficient ρ are the same for all genotypes.

Next, we calculate the mean fitness trajectories $F_1(t)$ and $F_2(t)$ in the home and non-home environments, respectively. To calculate $F_1(t)$, recall that the probability

$p(x, y, t; x_0, y_0)$ of observing the population at fitness (x, y) at time t, given that its fitness was (x_0, y_0) at time zero, obeys the Kolmogorov backward equation (in the diffusion approximation)

$$\frac{\partial p}{\partial t} = r_1 \frac{\partial p}{\partial x_0} + r_2 \frac{\partial p}{\partial y_0} + \frac{D_{11}}{2} \frac{\partial^2 p}{\partial x_0^2} + D_{12} \frac{\partial^2 p}{\partial x_0 \partial y_0} + \frac{D_{22}}{2} \frac{\partial^2 p}{\partial y_0^2}.$$

Multiplying it by x and integrating, we obtain an equation for the mean fitness $F_1(t; x_0)$ in the home environment

$$\frac{\partial F_1}{\partial t} = r_1(x_0) \frac{\partial F_1}{\partial x_0} + r_2(x_0) \frac{\partial F_1}{\partial y_0} + \frac{D_{11}(x_0)}{2} \frac{\partial^2 F_1}{\partial x_0^2} + D_{12}(x_0) \frac{\partial^2 F_1}{\partial x_0 \partial y_0} + \frac{D_{22}(x_0)}{2} \frac{\partial^2 F_1}{\partial y_0^2} \quad (14)$$

with the initial condition

$$F_1(0; x_0) = x_0. \quad (15)$$

In our model, the DFE in the home environment does not depend on the fitness in the non-home environment. Therefore F_1 does not depend on the initial fitness in the non-home environment y_0. Furthermore, we will assume that $\mu_1(x) \leq \mu_1(x_0) \ll 1$ so that the term $D_{11}(x_0)$ can be ignored compared to the term $r_1(x_0)$. Then, equation (21) simplifies to

$$\frac{\partial F_1}{\partial t} = r_1(x_0) \frac{\partial F_1}{\partial x_0}, \quad (16)$$

which can be solved by the method of characteristics. An alternative way to solve it is to use the result from Ref. (Kryazhimskiy et al., 2009) where it is shown that equation (23) is equivalent to the ordinary differential equation

$$\dot{F}_1 = r_1 \left(F_1 \right) \quad (17)$$

with the initial condition (22). The solution of equations (23), (24) is

$$F_1 = x_{\max} - \left[2\gamma_1^2 \, t + \frac{1}{x_{\max} - x_0} \right]^{-1}. \quad (18)$$

As expected, $F_1(t; x_0) \to x_{\max}$ as $t \to \infty$, i.e., up to the maximum fitness where beneficial mutations are still available.

To calculate $F_2(t)$, recall that the probability $p(x, y, t; x_0, y_0)$ also obeys the Fokker-Planck equation

$$\frac{\partial p}{\partial t} = -\frac{\partial}{\partial x} \left(r_1 \, p \right) - \frac{\partial}{\partial y} \left(r_2 \, p \right) + \frac{1}{2} \frac{\partial^2}{\partial x^2} \left(D_{11} \, p \right) + \frac{\partial^2}{\partial x \partial y} \left(D_{12} \, p \right) + \frac{1}{2} \frac{\partial^2}{\partial y^2} \left(D_{22} \, p \right).$$

Multiplying it by y and integrating, we obtain an integro-differential equation for F_2, which to the leading order $O(\mu_1)$, is approximated by the ODE

$$\dot{F}_2 = \langle r_2 \rangle \, (t), \quad (19)$$

with the initial condition

$$F_2(0) = y_0, \tag{20}$$

where

$$\langle r_2 \rangle (t) = \int_{\mathbb{R}^+} r_2(x)\, dx \int_{\mathbb{R}} p(x, y, t)\, dy = \gamma_1 \left(\mu_2 + \rho\,\sigma\right) \left(x_{\max} - F_1(t)\right) \tag{21}$$

is the r_2 expected at time t. Substituting expressions (25) and (28) into (26) and integrating, we obtain

$$F_2 = y_0 + \frac{\mu_2 + \rho\,\sigma}{2\gamma_1} \ln\left[1 + 2\gamma_1^2 \left(x_{\max} - x_0\right) t\right]. \tag{22}$$

Equations (25) and (29) are the theoretical predictions plotted in Figure 3.

Generation of JDFEs

Gaussian JDFEs. The JDFEs in Figure 1 have the following parameters. Mean in the home environment: -0.1. Standard deviation in both home and non-home environments: 0.1. Means in the non-home environment: 0.08, 0.18, 0, -0.18, -0.08 in panels A through E, respectively.

The JDFEs in Figure 2 have the following parameters. Mean and standard deviation in the home environment: -0.1 and 0.1, respectively. The non-home mean varies between -0.15 and 0.05. The non-home standard deviation varies between 0.06 and 0.1. The correlation between home and non-home fitness varies between -0.9 and 0.9. All parameter values and the resulting pleiotropy statistics for these JDFEs are given in the Supplementary Table S1.

JDFEs with equal probabilities of pleiotropically beneficial and deleterious mutations. All JDFEs in Figure S1 are mixtures of two two-dimensional uncorrelated Gaussian distributions, which have the following parameters. Mean in the home environment: 0.4. Standard deviation in both home and non-home environments: 0.1. Means in the non-home environment: 0.1 and -0.1 in panel A, 0.5 and -0.5 in panel B, 0.17 and -0.5 in panel C, and 0.5 and -0.17 in panel D.

JDFEs with epistasis. The JDFEs used in Figure 3 are given by equations (12) and (20). In all panels, $\mu_2 = -0.1$, $\sigma = 0.01$, $x_{\max} = 3$ and $\rho = -0.9$. Parameter γ equals 0.05, 0.05, 0.025, 0.0125 in panels E through H, respectively. JDFEs in panels I through L retain the same parameters as in panels E through H, respectively, with the exception that ρ which varies from -0.9 to 0.9 in increments of 0.2.

Antibiotic resistance koJDFEs. We draw random mutations from the *E. coli* antibiotic resistance koJDFE as follows. We first determined that the distributions of measured knock-out (KO) growth rates in the presence of antibiotics were best approximated by the Weibull distribution (Supplementary Table S5). To draw the selection coefficient of a new mutation in a given home environment, we sample from the Weibull distribution fitted to that environment and subtract the corresponding wildtype growth rate. We next drew the selection coefficient of this mutation in the non-home environment from the conditional distribution, which we obtain as follows. In each home environment, we bin all knock-out mutations by their home growth rate into 13 bins of size 0.1. For each bin, we fit the Weibull distribution to the non-home growth rates of all mutants that fall into the bin (Supplementary Table S6). We find the bin that corresponding to the new mutation and draw a random number from the fitted conditional distribution to obtain (after subtracting wildtype growth rate) the mutant's non-home selection coefficient. Finally, if the selection coefficient of the mutation in the home environment is above s_α^- and below s_α^+ (specified below in the section "Identification of resistant, collaterally resistant and collaterally sensitive mutations"), the mutation is considered neutral in the home environment, and its home selection coefficient is set to zero.

Simulations

We carried out two types of simulations, SSWM model simulations and full Wright-Fisher model simulations.

Strong selection weak mutation

The SSWM simulations were carried out using the Gillespie algorithm (Gillespie, 1976), as follows. We initiate the populations with home and non-home fitness values $x_0 = 1$ and $y_0 = 1$. At each iteration, we draw the waiting time until the appearance of the next beneficial mutation from the exponential distribution with the rate parameter NU_b and advance the time by this amount. Then, we draw the selection coefficients Δx and Δy of this mutation in the home- and non-home environment, respectively, from the JDFE (see below for the explanation of how we draw from the antibiotic resistance JDFEs). With probability $2\Delta x$, the mutation fixes in the population. If it does, the fitness of the population is updated accordingly.

Wright-Fisher model

We simulate evolution in the home environment according to the Wright-Fisher model with population size N as follows. We initiate the whole population with a single genotype with fitness $x_0 = 1$ and $y_0 = 1$ in the home and non-home environments, except for simulations with epistasis (see below). Suppose that at generation t, there are $K(t)$ genotypes, such that genotype i has home- and non-home fitness X_i and Y_i, respectively,

and it is present at frequency $f_i(t) > 0$ in the population. We generate the genotype frequencies at generation $t+1$ in three steps. In the reproduction step, we draw $B_i'(t+1)$, $i = 1, ..., K(t)$ from the multinomial distribution with the number of trials N and success probabilities $p_i(t) = f_i(t) + f_i(t)\left(X_i(t) - \overline{X}(t)\right)$, where $\overline{X}(t) = \sum_{i=1}^{K(t)} X_i(t) f_i(t)$ is the mean fitness of the population in the home environment at generation t. In the mutation step, we draw the number M of new mutants from the Poisson distribution with parameter NU, where U is the total per individual per generation mutation rate. We randomly determine the "parent" genotypes in which each mutation occurs and turn the appropriate numbers of parent individuals into new mutants. We assume that each new mutant has a new genotype (infinite alleles model). To obtain the new genotype's home and non-home fitness, we first draw its selection coefficients in the home and non-home environments from its JDFE (see below for the explanation of how we draw from the antibiotic resistance JDFEs) and then add these selection coefficients to the parent genotype's fitness. In the final step, all genotypes which are represented by zero individuals are removed and we are left with $K(t+1)$ genotypes with $B_i(t+1) > 0$, $i = 1, \ldots, K(t+1)$ individuals. Then we set $f_i(t+1) = B_i(t+1)/N$.

Simulations on JDFEs with epistasis. Since we initiate our Wright-Fisher simulations with monomorphic populations, it takes some time for these populations to accumulate diversity. This creates a 'lag' before the mean fitness of the population begins to change. The lag effectively shifts the entire ensemble of simulated fitness trajectories to the right relative to theoretical predictions which cannot have such lag by construction. This lag becomes especially pronounced in simulations with epistasis. To resolve this issue, we initiate all populations at home fitness $x_0 = 0.5$ $y_0 = 0.5$ and evolve them for a "burn-in" period until the mean population fitness in the home environment reaches 1. This burn-in period usually takes between 50 and 200 generations. Figure 3 shows the trajectories after the burn-in period.

Analysis of the antibiotic resistance koJDFEs

Identification of resistant, collaterally resistant and collaterally sensitive mutations

We identified resistance mutations in a given antibiotic environment as those that were significantly more beneficial than would be expected due to measurement errors. To do so, we obtained the wildtype growth rate measurements in the presence of antibiotics from Guillaume Chevereau and Tobias Bollenbach (available at https://github.com/ardellsarah/JDFE-project). In this data set, the wildtype *E. coli* strain is measured on average 476 times. In each environment, we estimate the wildtype growth rate r_{WT} as the mean of these measurements. We then shift all growth rate measurements (for the wildtype and the mutants) in that environment by r_{WT} and thereby obtain the selection

coefficient $s_i = r_i - r_{\mathrm{WT}}$ for each knock-out i as well as the "noise distribution" $P_{\mathrm{noise}}(s)$, that is the probability of observing selection coefficient s simply due to noise. $P_{\mathrm{noise}}(s)$ is shown in red in the diagonal panels in Figure 4.

The noise distribution allows us to identify the critical selection coefficient $s_\alpha^+ > 0$, such that any discovered beneficial knock-out mutation (i.e., any mutation i with $s_i \geq s_\alpha^+$) has the probability α of being a false positive (i.e., not beneficial). Thus, for any α, we calculate the expected false discovery rate (FDR) among discovered beneficial mutations as

$$\mathrm{FDR}_{\mathrm{ben}}(\alpha) = \alpha \times \frac{\#\text{ of mutations with } s_i > 0}{\#\text{ of mutations with } s_i > s_\alpha^+}.$$

We similarly identify the critical value s_α^- and the FDR for deleterious mutations.

For each antibiotic, we attempt to find such α that $\mathrm{FDR}_{\mathrm{ben}}(\alpha) \approx 0.25$. We could not find such α in the trimethoprim (TMP) and chloramphenicol (CHL) environments, i.e., there were not enough knock-out mutations with positive selection coefficients to reliably distinguish them from measurement errors. We also carry out the same procedure with $\mathrm{FDR}_{\mathrm{ben}}(\alpha) \approx 0.5$.

To identify mutations resistant against drug A that were also collaterally resistant against drug B, we applied the same procedure as described above, only restricted to the pool of mutations identified as resistant to drug A and aiming for FDR $\lesssim 0.05$. We called collaterally sensitive mutations analogously.

Estimation of the pleiotropy statistics from a sample of mutations

To estimate the pleiotropy statistics for a given pair of home and non-home environments, we first identify the subset of mutations that are beneficial in the home environment. Denoting the effects of these mutations in the home and non-home environments by Δx and Δy, respectively, we estimate the pleiotropy statistics as $\hat{r}_1 = \overline{(\Delta x)^2}$, $\hat{r}_2 = \overline{\Delta x\, \Delta y}$, $\hat{D}_{11} = \overline{(\Delta x)^3}$, $\hat{D}_{12} = \overline{(\Delta x)^2\, \Delta y}$, $\hat{D}_{22} = \overline{\Delta x\, (\Delta y)^2}$, where the overline denotes an average over beneficial mutations.

Implementation

All code was written in R. Distributions were fit using the `fitdistrplus` package. Linear models were fit using the `lm` function. All scripts are available at https://github.com/ardellsarah/JDFE-project.

Acknowledgements

We thank Shea Summers and Flora Tang for help and input at the initial stages of the project and Kryazhimskiy and Meyer labs for feedback. We thank Tobias Bollenbach and

Guillaume Chevereau for providing wildtype growth rate measurement data. This work was supported by the BWF Career Award at Scientific Interface (Grant 1010719.01), the Alfred P. Sloan Foundation (Grant FG-2017-9227), the Hellman Foundation and NIH (Grant 1R01GM137112).

References

Aggeli, D., Y. Li and G. Sherlock. 2020. Changes in the distribution of fitness effects and adaptive mutational spectra following a single first step towards adaptation. bioRxiv: 2020.06.12.148833 URL https://doi.org/10.1101/2020.06.12.148833.

Anderson, J. T., J. H. Willis and T. Mitchell-Olds. 2011. Evolutionary genetics of plant adaptation. Trends in Genetics **27**:258–266.

Andersson, D. I. and D. Hughes. 2010. Antibiotic resistance and its cost: is it possible to reverse resistance? Nature Reviews Microbiology **8**:260–271.

Barbosa, C., V. Trebosc, C. Kemmer, P. Rosenstiel, R. Beardmore, H. Schulenburg and G. Jansen. 2017. Alternative evolutionary paths to bacterial antibiotic resistance cause distinct collateral effects. Molecular biology and evolution **34**:2229–2244.

Barton, N. 1990. Pleiotropic models of quantitative variation. Genetics **124**:773–782.

Bedhomme, S., J. Hillung and S. F. Elena. 2015. Emerging viruses: why they are not jacks of all trades? Current opinion in virology **10**:1–6.

Bergstrom, C. T., M. Lo and M. Lipsitch. 2004. Ecological theory suggests that antimicrobial cycling will not reduce antimicrobial resistance in hospitals. Proceedings of the National Academy of Sciences **101**:13285–13290.

Blundell, J. R., K. Schwartz, D. Francois, D. S. Fisher, G. Sherlock and S. F. Levy. 2019. The dynamics of adaptive genetic diversity during the early stages of clonal evolution. Nature ecology & evolution **3**:293–301.

Bonhoeffer, S., M. Lipsitch and B. R. Levin. 1997. Evaluating treatment protocols to prevent antibiotic resistance. Proceedings of the National Academy of Sciences **94**:12106–12111.

Bono, L. M., L. B. Smith Jr, D. W. Pfennig and C. L. Burch. 2017. The emergence of performance trade-offs during local adaptation: insights from experimental evolution. Molecular ecology **26**:1720–1733.

Card, K. J., M. D. Thomas, J. L. Graves Jr, J. E. Barrick and R. E. Lenski. 2020. Genomic evolution of antibiotic resistance is contingent on genetic background following a long-term experiment with *Escherichia coli*. bioRxiv: 2020.08.19.258384 URL https://doi.org/10.1101/2020.08.19.258384.

Chevereau, G., M. Dravecká, T. Batur, A. Guvenek, D. H. Ayhan, E. Toprak and T. Bollenbach. 2015. Quantifying the determinants of evolutionary dynamics leading to drug resistance. PLoS Biology **13**:e1002299.

Chiang, G. C., D. Barua, E. Dittmar, E. M. Kramer, R. R. De Casas and K. Donohue. 2013. Pleiotropy in the wild: the dormancy gene *DOG1* exerts cascading control on life cycles. Evolution **67**:883–893.

Chou, H.-H., H.-C. Chiu, N. F. Delaney, D. Segrè and C. J. Marx. 2011. Diminishing returns epistasis among beneficial mutations decelerates adaptation. Science **332**:1190–1192.

Connallon, T. and A. G. Clark. 2015. The distribution of fitness effects in an uncertain world. Evolution **69**:1610–1618.

Crow, J. F. and M. Kimura. 1972. An introduction to population genetics theory. Harper & Row Ltd.

Das, S. G., S. O. Direito, B. Waclaw, R. J. Allen and J. Krug. 2020. Predictable properties of fitness landscapes induced by adaptational tradeoffs. eLife **9**:e55155.

Desai, M. M. and D. S. Fisher. 2007. Beneficial mutation–selection balance and the effect of linkage on positive selection. Genetics **176**:1759–1798.

D'Souza, G., S. Waschina, S. Pande, K. Bohl, C. Kaleta and C. Kost. 2014. Less is more: selective advantages can explain the prevalent loss of biosynthetic genes in bacteria. Evolution **68**:2559–2570.

Duffy, S., P. E. Turner and C. L. Burch. 2006. Pleiotropic costs of niche expansion in the rna bacteriophage ϕ6. Genetics **172**:751–757.

Elena, S. F. 2017. Local adaptation of plant viruses: lessons from experimental evolution. Molecular Ecology **26**:1711–1719.

Eyre-Walker, A. and P. D. Keightley. 2007. The distribution of fitness effects of new mutations. Nature Reviews Genetics **8**:610–618.

Forister, M., L. A. Dyer, M. Singer, J. O. Stireman III and J. Lill. 2012. Revisiting the evolution of ecological specialization, with emphasis on insect–plant interactions. Ecology **93**:981–991.

Friberg, M., M. Bergman, J. Kullberg, N. Wahlberg and C. Wiklund. 2008. Niche separation in space and time between two sympatric sister species—a case of ecological pleiotropy. Evolutionary Ecology **22**:1–18.

Futuyma, D. J. and G. Moreno. 1988. The evolution of ecological specialization. Annual review of Ecology and Systematics **19**:207–233.

Gillespie, D. T. 1976. A general method for numerically simulating the stochastic time evolution of coupled chemical reactions. Journal of computational physics **22**:403–434.

Good, B. H. and M. M. Desai. 2015. The impact of macroscopic epistasis on long-term evolutionary dynamics. Genetics **199**:177–190.

Good, B. H., M. J. McDonald, J. E. Barrick, R. E. Lenski and M. M. Desai. 2017. The dynamics of molecular evolution over 60,000 generations. Nature **551**:45–50.

Good, B. H., I. M. Rouzine, D. J. Balick, O. Hallatschek and M. M. Desai. 2012. Distribution of fixed beneficial mutations and the rate of adaptation in asexual populations. Proceedings of the National Academy of Sciences **109**:4950–4955.

Hall, M. D., M. D. Handley and M. M. Gottesman. 2009. Is resistance useless? Multidrug resistance and collateral sensitivity. Trends in pharmacological sciences **30**:546–556.

Harmand, N., R. Gallet, R. Jabbour-Zahab, G. Martin and T. Lenormand. 2017. Fisher's geometrical model and the mutational patterns of antibiotic resistance across dose gradients. Evolution **71**:23–37.

Hietpas, R. T., C. Bank, J. D. Jensen and D. N. Bolon. 2013. Shifting fitness landscapes in response to altered environments. Evolution **67**:3512–3522.

Hottes, A. K., P. L. Freddolino, A. Khare, Z. N. Donnell, J. C. Liu and S. Tavazoie. 2013. Bacterial adaptation through loss of function. PLoS Genet **9**:e1003617.

Husain, K. and A. Murugan. 2020. Physical constraints on epistasis. Molecular Biology and Evolution URL https://doi.org/10.1093/molbev/msaa124. In press.

Hutchison, D. J. 1963. Cross resistance and collateral sensitivity studies in cancer chemotherapy. In Advances in cancer research, vol. 7, 235–350. Elsevier.

Imamovic, L. and M. O. Sommer. 2013. Use of collateral sensitivity networks to design drug cycling protocols that avoid resistance development. Science translational medicine **5**:204ra132.

Jensen, P., B. Holm, M. Sorensen, I. Christensen and M. Sehested. 1997. In vitro cross-resistance and collateral sensitivity in seven resistant small-cell lung cancer cell lines: preclinical identification of suitable drug partners to taxotere, taxol, topotecan and gemcitabin. British journal of cancer **75**:869–877.

Jerison, E. R., S. Kryazhimskiy and M. M. Desai. 2014. Pleiotropic consequences of adaptation across gradations of environmental stress in budding yeast. arXiv:1409.7839 URL https://arxiv.org/abs/1409.7839.

Jerison, E. R., A. N. Nguyen Ba, M. M. Desai and S. Kryazhimskiy. 2020. Chance and necessity in the pleiotropic consequences of adaptation for budding yeast. Nature Ecology & Evolution **4**:601–611.

Johnson, M. S., A. Martsul, S. Kryazhimskiy and M. M. Desai. 2019. Higher-fitness yeast genotypes are less robust to deleterious mutations. Science **366**:490–493.

Johnson, T. and N. Barton. 2005. Theoretical models of selection and mutation on quantitative traits. Philosophical Transactions of the Royal Society B: Biological Sciences **360**:1411–1425.

Jones, A. G., S. J. Arnold and R. Bürger. 2003. Stability of the g-matrix in a population experiencing pleiotropic mutation, stabilizing selection, and genetic drift. Evolution **57**:1747–1760.

Khan, A. I., D. M. Dinh, D. Schneider, R. E. Lenski and T. F. Cooper. 2011. Negative epistasis between beneficial mutations in an evolving bacterial population. Science **332**:1193–1196.

Kimura, M. 1962. On the probability of fixation of mutant genes in a population. Genetics **47**:713.

King, J. L. 1972. The role of mutation in evolution. In Proceedings of the Sixth Berkeley Symposium on Mathematical Statistics and Probability, vol. 5, 69–100. University of California Press Berkeley.

Kinsler, G., K. Geiler-Samerotte and D. A. Petrov. 2020. A genotype-phenotype-fitness map reveals local modularity and global pleiotropy of adaptation. bioRxiv: 2020.06.25.172197 URL https://doi.org/10.1101/2020.06.25.172197.

Kohanski, M. A., D. J. Dwyer, B. Hayete, C. A. Lawrence and J. J. Collins. 2007. A common mechanism of cellular death induced by bactericidal antibiotics. Cell **130**:797–810.

Kryazhimskiy, S., D. P. Rice, E. R. Jerison and M. M. Desai. 2014. Global epistasis makes adaptation predictable despite sequence-level stochasticity. Science **344**:1519–1522.

Kryazhimskiy, S., G. Tkačik and J. B. Plotkin. 2009. The dynamics of adaptation on correlated fitness landscapes. Proceedings of the National Academy of Sciences **106**:18638–18643.

Lahti, D. C., N. A. Johnson, B. C. Ajie, S. P. Otto, A. P. Hendry, D. T. Blumstein, R. G. Coss, K. Donohue and S. A. Foster. 2009. Relaxed selection in the wild. Trends in ecology & evolution **24**:487–496.

Lande, R. and S. J. Arnold. 1983. The measurement of selection on correlated characters. Evolution **37**:1210–1226.

Lang, G. I., D. P. Rice, M. J. Hickman, E. Sodergren, G. M. Weinstock, D. Botstein and M. M. Desai. 2013. Pervasive genetic hitchhiking and clonal interference in forty evolving yeast populations. Nature **500**:571–574.

Lázár, V., A. Martins, R. Spohn, L. Daruka, G. Grézal, G. Fekete, M. Számel, P. K. Jangir, B. Kintses, B. Csörgő et al. 2018. Antibiotic-resistant bacteria show widespread collateral sensitivity to antimicrobial peptides. Nature microbiology **3**:718–731.

Lee, C. E. 2002. Evolutionary genetics of invasive species. Trends in ecology & evolution **17**:386–391.

Lenski, R. E. 1988. Experimental studies of pleiotropy and epistasis in *Escherichia coli*. *I*. Variation in competitive fitness among mutants resistant to virus T4. Evolution **42**:425–432.

Levy, S. F., J. R. Blundell, S. Venkataram, D. A. Petrov, D. S. Fisher and G. Sherlock. 2015. Quantitative evolutionary dynamics using high-resolution lineage tracking. Nature **519**:181–186.

Li, Y., D. A. Petrov and G. Sherlock. 2019. Single nucleotide mapping of trait space reveals pareto fronts that constrain adaptation. Nature ecology & evolution **3**:1539–51.

Lindsey, H. A., J. Gallie, S. Taylor and B. Kerr. 2013. Evolutionary rescue from extinction is contingent on a lower rate of environmental change. Nature **494**:463–467.

Lukačišinová, M., B. Fernando and T. Bollenbach. 2020. Highly parallel lab evolution reveals that epistasis can curb the evolution of antibiotic resistance. Nature communications **11**:1–14.

MacLean, R. C. and A. Buckling. 2009. The distribution of fitness effects of beneficial mutations in *Pseudomonas aeruginosa*. PLoS Genet **5**:e1000406.

Maltas, J., D. M. McNally and K. B. Wood. 2019. Evolution in alternating environments with tunable inter-landscape correlations. bioRxiv: 803619 URL https://doi.org/10.1101/803619.

Maltas, J. and K. B. Wood. 2019. Pervasive and diverse collateral sensitivity profiles inform optimal strategies to limit antibiotic resistance. PLoS Biology **17**:e3000515.

Martin, G. and T. Lenormand. 2008. The distribution of beneficial and fixed mutation fitness effects close to an optimum. Genetics **179**:907–916.

———. 2015. The fitness effect of mutations across environments: Fisher's geometrical model with multiple optima. Evolution **69**:1433–1447.

Masterton, R. G. 2005. Antibiotic cycling: more than it might seem? Journal of antimicrobial chemotherapy **55**:1–5.

Mira, P. M., J. C. Meza, A. Nandipati and M. Barlow. 2015. Adaptive landscapes of resistance genes change as antibiotic concentrations change. Molecular biology and evolution **32**:2707–2715.

Morin, M., E. C. Pierce and R. J. Dutton. 2018. Changes in the genetic requirements for microbial interactions with increasing community complexity. eLife **7**:e37072.

Nichol, D., J. Rutter, C. Bryant, A. M. Hujer, S. Lek, M. D. Adams, P. Jeavons, A. R. Anderson, R. A. Bonomo and J. G. Scott. 2019. Antibiotic collateral sensitivity is contingent on the repeatability of evolution. Nature communications **10**:1–10.

Ohta, T. 1987. Very slightly deleterious mutations and the molecular clock. Journal of Molecular Evolution **26**:1–6.

Orr, H. A. 2000. The rate of adaptation in asexuals. Genetics **155**:961–968.

———. 2003. The distribution of fitness effects among beneficial mutations. Genetics **163**:1519–1526.

Ostrowski, E. A., D. E. Rozen and R. E. Lenski. 2005. Pleiotropic effects of beneficial mutations in *Escherichia coli*. Evolution **59**:2343–2352.

Otto, S. P. 2004. Two steps forward, one step back: the pleiotropic effects of favoured alleles. Proceedings of the Royal Society of London. Series B: Biological Sciences **271**:705–714.

Oz, T., A. Guvenek, S. Yildiz, E. Karaboga, Y. T. Tamer, N. Mumcuyan, V. B. Ozan, G. H. Senturk, M. Cokol, P. Yeh et al. 2014. Strength of selection pressure is an important parameter contributing to the complexity of antibiotic resistance evolution. Molecular biology and evolution **31**:2387–2401.

Pál, C., B. Papp and V. Lázár. 2015. Collateral sensitivity of antibiotic-resistant microbes. Trends in microbiology **23**:401–407.

Pinheiro, F., O. Warsi, D. I. Andersson and M. Lässig. 2020. Predicting trajectories and mechanisms of antibiotic resistance evolution. arXiv:2007.01245 URL https://arxiv.org/abs/2007.01245.

Pluchino, K. M., M. D. Hall, A. S. Goldsborough, R. Callaghan and M. M. Gottesman. 2012. Collateral sensitivity as a strategy against cancer multidrug resistance. Drug Resistance Updates **15**:98–105.

Qian, W., D. Ma, C. Xiao, Z. Wang and J. Zhang. 2012. The genomic landscape and evolutionary resolution of antagonistic pleiotropy in yeast. Cell reports **2**:1399–1410.

Reddy, G. and M. M. Desai. 2020. Global epistasis emerges from a generic model of a complex trait. bioRxiv: 2020.06.14.150946 URL https://www.biorxiv.org/content/early/2020/06/14/2020.06.14.150946.

Rees, K. and T. Bataillon. 2006. Distribution of fitness effects among beneficial mutations before selection in experimental populations of bacteria. Nature Genetics **38**:484–488.

Reusch, H. and T. Woody. 2007. Molecular ecology of climate change. Mol. Ecol **16**:3973–3992.

Rodríguez-Verdugo, A., D. Carrillo-Cisneros, A. González-González, B. S. Gaut and A. F. Bennett. 2014. Different tradeoffs result from alternate genetic adaptations to a common environment. Proceedings of the National Academy of Sciences **111**:12121–12126.

Roemhild, R., M. Linkevicius and D. I. Andersson. 2020. Molecular mechanisms of collateral sensitivity to the antibiotic nitrofurantoin. PLoS Biology **18**:e3000612.

Roff, D. A. and D. Fairbairn. 2007. The evolution of trade-offs: where are we? Journal of evolutionary biology **20**:433–447.

Rose, M. R. 1982. Antagonistic pleiotropy, dominance, and genetic variation. Heredity **48**:63–78.

Schurek, K. N., A. K. Marr, P. K. Taylor, I. Wiegand, L. Semenec, B. K. Khaira and R. E. Hancock. 2008. Novel genetic determinants of low-level aminoglycoside resistance in *Pseudomonas aeruginosa*. Antimicrobial Agents and Chemotherapy **52**:4213–4219.

Shoval, O., H. Sheftel, G. Shinar, Y. Hart, O. Ramote, A. Mayo, E. Dekel, K. Kavanagh and U. Alon. 2012. Evolutionary trade-offs, Pareto optimality, and the geometry of phenotype space. Science **336**:1157–1160.

Slatkin, M. and S. A. Frank. 1990. The quantitative genetic consequences of pleiotropy under stabilizing and directional selection. Genetics **125**:207–213.

Tenaillon, O., A. Rodríguez-Verdugo, R. L. Gaut, P. McDonald, A. F. Bennett, A. D. Long and B. S. Gaut. 2012. The molecular diversity of adaptive convergence. Science **335**:457–461.

Tikhonov, M., S. Kachru and D. S. Fisher. 2020. A model for the interplay between plastic tradeoffs and evolution in changing environments. Proceedings of the National Academy of Sciences **117**:8934–8940.

Török, M., N. Chantratita and S. Peacock. 2012. Bacterial gene loss as a mechanism for gain of antimicrobial resistance. Current opinion in microbiology **15**:583–587.

Travisano, M. and R. E. Lenski. 1996. Long-term experimental evolution in *Escherichia coli*. IV. Targets of selection and the specificity of adaptation. Genetics **143**:15–26.

Van Kampen, N. G. 1992. Stochastic processes in physics and chemistry, vol. 1. Elsevier.

Van Opijnen, T., K. L. Bodi and A. Camilli. 2009. Tn-seq: high-throughput parallel sequencing for fitness and genetic interaction studies in microorganisms. Nature methods **6**:767–772.

Venkataram, S., B. Dunn, Y. Li, A. Agarwala, J. Chang, E. R. Ebel, K. Geiler-Samerotte, L. Hérissant, J. R. Blundell, S. F. Levy et al. 2016. Development of a comprehensive genotype-to-fitness map of adaptation-driving mutations in yeast. Cell **166**:1585–1596.

Wang, S. and L. Dai. 2019. Evolving generalists in switching rugged landscapes. PLoS Comput Biology **15**:e1007320.

Wang, Y., C. D. Arenas, D. M. Stoebel, K. Flynn, E. Knapp, M. M. Dillon, A. Wünsche, P. J. Hatcher, F. B.-G. Moore, V. S. Cooper et al. 2016. Benefit of transferred mutations is better predicted by the fitness of recipients than by their ecological or genetic relatedness. Proceedings of the National Academy of Sciences **113**:5047–5052.

Wetmore, K. M., M. N. Price, R. J. Waters, J. S. Lamson, J. He, C. A. Hoover, M. J. Blow, J. Bristow, G. Butland, A. P. Arkin et al. 2015. Rapid quantification of mutant fitness in diverse bacteria by sequencing randomly bar-coded transposons. mBio **6**:e00306–15.

Wiser, M. J., N. Ribeck and R. E. Lenski. 2013. Long-term dynamics of adaptation in asexual populations. Science **342**:1364–1367.

Supplementary Figures

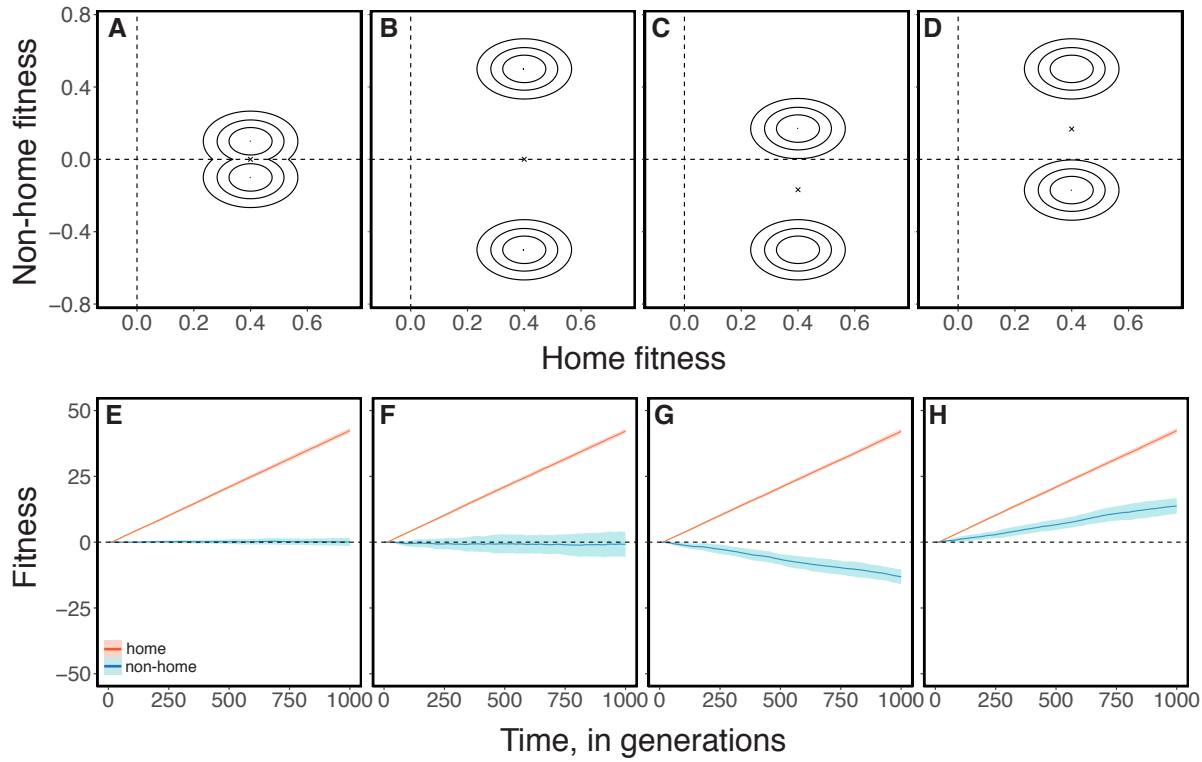

Supplementary Figure S1. Same as Figure 1, but for JDFEs with equal probability weights in the first and fourth quadrants. See Materials and Methods for details.

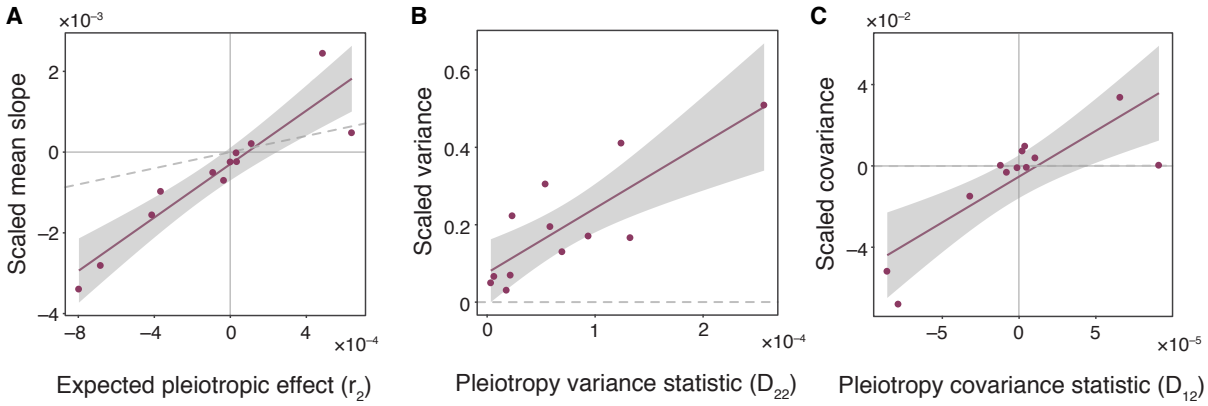

Supplementary Figure S2. Same as Figure 2, but for *E. coli* antibiotic resistance koJDFEs (see Materials and Methods for details). Evolution was simulated using the Wright-Fisher model with $N = 10^4$ and $U = 10^{-2}$. $P < 0.01$ for all linear regressions.

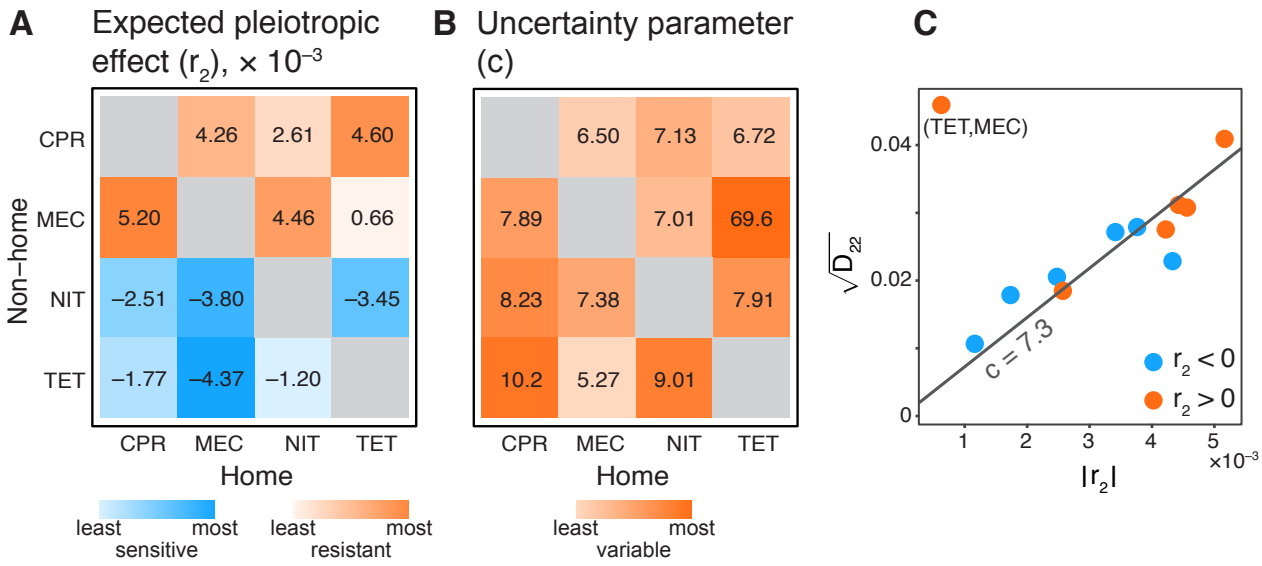

Supplementary Figure S3. Same as Figure 5, but with parameters estimated from reistance mutations discovered at 50% FDR.

Supplementary Tables

Supplementary table S1. Parameters of Gaussian JDFEs without epistasis, used in Figure 2.

Supplementary table S2. Knock-out mutations identified as significantly beneficial (2), deleterious (1), or neutral (0) at 25% FDR in each of four drugs.

Supplementary table S3. Mean, variance, covariance and pleiotropy statistics for all antibiotic resistance koJDFEs, calculated with beneficial knock-out mutations discovered at 25% FDR.

Supplementary table S4. Mean, variance, covariance and pleiotropy statistics for all antibiotic resistance koJDFEs, calculated with beneficial knock-out mutations discovered at 50% FDR.

	Fitted distribution		
Home	Weibull	Gaussian	Exponential
CPR	2838	2471	−3553
MEC	1237	1141	−3289
NIT	4846	3705	−3592
TET	4879	3705	−3507

Supplementary table S5. Log likelihood values for different distributions fitted to home DFEs. Higher values signify better fit.

Supplementary table S6. The shape and scale parameters for the home DFEs and conditional non-home DFEs in all home/non-home antibiotic pairs. N/A values represent empty bins.